



The Professional Journal of the
Earthquake Engineering Research Institute



[Home](#) [Browse](#) [Special Issues](#) [About](#) [Authors](#) [EERI](#) [Email Alerts](#) [Help](#)

[Home](#) > [Earthquake Spectra](#) > December 2000

[Advanced Search](#)

Volume 16, Issue S1
(December 2000)

Volume 16, Issue S1 (December 2000)

[< Previous](#) [Next >](#)



[Current Issue](#)
[Available Issues](#)
[Preprints](#)

Alerts for the Journal

Click [here](#) to get an email alert for every new issue of

Earthquake Spectra

Journal Information

ISSN: 8755-2930

Frequency: Quarterly

Register for a Profile

Not Yet [Registered?](#)

Benefits of Registration Include:

- A Unique User Profile that will allow you to manage your current subscriptions (including online access)
- The ability to create favorites lists down to the article level
- The ability to customize email alerts to receive specific notifications about the topics you care most about and special offers

[Register Now!](#)

[View Abstracts](#)

[Add to Favorites](#)

[Share Article](#)

[Export Citations](#)

Track Citations ([RSS](#) | [Email](#))

☐ Select All

☐ Open access

☐ Full access

☐ Partial access

☐ No access

xi ☐ PREFACE

[Citation](#) | [PDF \(269 KB\)](#)

1 ☐ Geology and Seismicity

W. Lettis, J. Bachhuber, A. Barka, C. Brankman, W. Lettis, P. Somerville and R. Witter

[Citation](#) | [PDF \(862 KB\)](#)

11 ☐ Surface Fault Rupture

W. Lettis, J. Bachhuber, R. Witter, J. Bachhuber, A. Barka, J. Bray, W. Lettis, W. Page, F. Swan, R. Witter, E. Altunel, J.-P. Bardet, R. Boulanger, C. Brankman and Z. Cakir

[Citation](#) | [PDF \(8160 KB\)](#)

55 ☐ Tsunami Waves in Izmit Bay

Ahmet Cevdet Yalciner, Yildiz Altinok, Costas E. Synolakis, Jose Borrero, Fumihiko Imamura, Sukru Ersoy, Ugur Kuran, Stefano Tinti, Martin Eshkjian, John Freikman, Yalcin Yuksel, Bedri Alpar, Philip Watts, Utku Kanoglu and Jean-Pierre Bardet

[Citation](#) | [PDF \(1225 KB\)](#)

65 ☐ Strong Ground Motions and Site Effects

E. Rathje, I.M. Idriss, E. Rathje, P. Somerville, A. Ansal, J. Bachhuber, M. Baturay, M. Erdik, D. Frost, W. Lettis, B. Sozer, J. Stewart and T. Ugras

[Citation](#) | [PDF \(2763 KB\)](#)

97 ☐ Recorded Main Shock and Aftershock Motions

Erdal Safak, Mustafa Erdik, Kemal Beyen, David Carver, Edward Cranswick, Mehmet Celebi, Eser Durukal, William Ellsworth, Mustafa Erdik, Thomas Holzer, Mark Meremonte, Charles Mueller, Oguz Ozel, Erdal Safak and Selcuk Toprak

[Citation](#) | [PDF \(1427 KB\)](#)

113 ☐ Implications for Seismic Hazard Analysis

John G. Anderson, Haluk Sucuoglu, Altug Erberik, Tolga Yilmaz, Engin Inan, Eser Durukal, Mustafa Erdik, Rasool Anoooshehpour, James N. Brune and Shean-Der Ni

[Citation](#) | [PDF \(1920 KB\)](#)

141 ☐ Soil Liquefaction, Landslides, and Subsidence

J. P. Bardet, R. B. Seed, K. O. Cetin, W. Lettis, E. Rathje, G. Rau, R. B. Seed, D. Ural, M. B. Baturay, R. W. Boulanger, J. D. Bray, D. Erten, D. Frost and A. Kaya

[Citation](#) | [PDF \(3384 KB\)](#)

163 ☐ Damage Patterns and Foundation Performance in Adapazari

J. D. Bray, J. P. Stewart, M. B. Baturay, T. Durgunoglu, A. Onalp, R. B. Sancio, J. P. Stewart, D. Ural, A. Ansal, J. B. Bardet, A. Barka, R. Boulanger, O. Cetin and D. Erten

[Citation](#) | [PDF \(3065 KB\)](#)

191 ☐ Performance of Improved Ground and Earth Structures

James K. Mitchell, James R. Martin II, C. Guney Olgun, Canan Emrem, H. Turan Durgunoglu and Turhan Karadayilar

[Citation](#) | [PDF \(3886 KB\)](#)

227 ☐ Effects on Dams









Ellis L. Krinitzsky, Mostafiz R. Chowdhury and Ghassan Al-Chaar

[Citation](#) | [PDF \(1017 KB\)](#)

237 ☐ Performance of Buildings

Mark Aschheim, Polat Gulkan, Halil Sezen, Michel Bruneau, Amr Elnashai, Marvin Halling, Jay Love and Mohsen Rahnama

[Citation](#) | [PDF \(6326 KB\)](#)

- 281 □ **Damage Survey Approach to Estimating Insurance Losses**
Laurie A. Johnson, Andrew Coburn, Mohsen Rahnema, Marvin Halling, Guy Morrow, Fouad Bendimerad and Ted Piepenbrock
[Citation](#) | [PDF \(1129 KB\)](#) 
- 295 □ **Performance of Waterfront Structures**
Ross W. Boulanger, Susumu Iai, Atilla Ansal, Kemal Onder Cetin, I. M. Idriss, Berna Sunman and Kivanc Sunman
[Citation](#) | [PDF \(3465 KB\)](#) 
- 311 □ **Industrial Facilities**
Gayle S. Johnson, Mark Aschheim and Halil Sezen
[Citation](#) | [PDF \(9473 KB\)](#) 
- 351 □ **Building Code Enforcement Prospects: The Failure of Public Policy**
Polat Gu'ikan
[Citation](#) | [PDF \(1467 KB\)](#) 
- 377 □ **Water, Gas, Electric Power, and Telecommunications Performance**
T. D. O'Rourke, Fakir Huseyin Erdogan, William U. Savage, Le Val Lund, Alex Tang, Nesrin Basoz, Curt Edwards, Gulcin Tezel and Felix Wong
[Citation](#) | [PDF \(2652 KB\)](#) 
- 403 □ **Performance of Transportation Systems After the 1999 Kocaeli Earthquake**
William G. Byers, Curt Edwards, Alex Tang, John Eidinger, Clifford Roblee, Mark Yashinsky, Jean-Pierre Bardet and Jennifer Swift
[Citation](#) | [PDF \(1345 KB\)](#) 
- 411 □ **Impact on Highway Structures**
R. A. Imbsen, C. J. Roblee, M. Yashinsky, M. M. Berilgen and S. Toprak
[Citation](#) | [PDF \(2703 KB\)](#) 
- 439 □ **Emergency Response and Societal Impacts**
William A. Mitchell
[Citation](#) | [PDF \(2365 KB\)](#) 

Published by **Earthquake Engineering Research Institute** with **Allen Press**.
Copyright © 2016 **Earthquake Engineering Research Institute**

2

Surface Fault Rupture

INTRODUCTION

Extensive surface rupture accompanied the August 17, 1999, Kocaeli earthquake. Surface rupture consisted primarily of right-lateral strike-slip displacement of up to 5.5 meters, averaging 3 to 4 meters, with localized vertical displacements of up to 2.4 meters. The fault rupture produced classic examples of strike-slip offset, including well-formed mole tracks, left-stepping *en echelon* fault traces at a variety of scales, uplift of pressure ridges, and subsidence of extensional pull-apart basins. Four distinct segments of the North Anatolian fault (NAF) ruptured during the earthquake, providing the opportunity to investigate the dynamic process of fault rupture and the physical and behavioral features of a fault that may control the propagation of fault rupture. Surface fault rupture traversed both rural and urban areas, generating excellent examples of the effects of surface fault rupture on engineered structures and, locally, the influence of some engineered structures on the surface expression of fault rupture.

This chapter describes the characteristics of surface fault rupture resulting from the August 17 earthquake. It covers the length of observed and inferred surface fault rupture, the distribution of horizontal and vertical displacements along the rupture zone, the fault segments and pull-apart basins involved in the rupture, and, lastly, the effects of surface fault rupture on the built environment.

SURFACE FAULT RUPTURE

RUPTURE LENGTH AND DISPLACEMENT

Surface rupture occurred over a distance of 126 km, extending westward from Eften Lake near the city of Düzce to the Hersek Peninsula in İzmit Bay (chapter 1, figure 1.5; plate 1). Fault rupture broke four distinct segments of the NAF: from east to west, the Karadere, Sakarya, Sapanca, and Gölcük segments (table 2.1). These segments range in length from 26 to 36 km and are bounded by right, *en echelon* stepovers and/or a gap in the fault trace. From east to west, the stepover and rupture gaps include Eften Lake stepover basin, Akyazi gap and restraining bend, Lake Sapanca stepover basin, Gölcük stepover basin, and Karamürsel stepover basin (plate 1; table 2.2). Surface mapping and seismicity focal mechanism solutions (e.g., chapter 1, figure 2.3; Kandilli Observatory 1999) show that fault rupture was nearly pure strike-slip. Surface displacements ranged from 1 to 1.5 meters on the Karadere segment, up to 4 meters on the Sapanca segment, and up to 5.5 meters on the Sakarya and Gölcük segments (e.g., Barka et al. 1999). Localized normal displacement of up to 2.4 meters occurred on a discrete normal fault along the southwest margin of the Gölcük pull-apart basin between the Gölcük and Sapanca fault segments.

These four fault segments are bounded on the west by the Yalova fault segment and on the east by the Düzce fault segment of the NAF. Minor surface faulting was observed or is suspected to have occurred on both these faults. The amount and extent of rupture on these segments adds uncertainty to the estimated total rupture length.

Table 2.1. Fault Segment Characteristics, August 17, 1999, Kocaeli (Izmit) Earthquake Rupture

| Segment | Length (km) | Orientation | Style | Offset (m) | | Fault Zone Width (m) | | | Rupture Expression | Geologic/ Topographic Setting |
|----------|----------------|-------------|------------------|-----------------------|----------------------------------|---------------------------------|-----------------------------------|--|---|---|
| | | | | Horizontal Max Avg | Vertical ¹ Max Avg | Primary ² Max Avg | Secondary ² Max Avg | | | |
| Gölcük | 29 | N78°E | right lateral | 5.5 3-5 | 2.4 1.2 | 30 10 | 60 35 | | 1 or 2 primary splays, sidehill scarp, moletrack, <i>en-echelon</i> tears. | Rupture occurs largely offshore. Segment Follows a straight reach of coastline and base of a small pressure ridge at the Gölcük Naval Base. Rupture primarily is within Holocene delta and alluvial deposits, fill. |
| Sapanca | 26 | N89°W | right lateral | 3.3 2-3 | 1.0 0.7 | 8 4 | 30 20 | | 1 or 2 primary splays, moletrack, sidehill scarps, <i>en-echelon</i> tears, sag ponds. | Rupture occurs across relatively flat alluvial valleys and across small ridges. Rupture primarily is within alluvial flood plain and terrace deposits and localized areas of colluvium and bedrock. |
| Sakarya | 36 | N87°W | right lateral | 5 2-4 | 0.5 0.3 | 20 10 | 200 100 | | 1 or 2 primary splays, moletrack, sidehill scarps, <i>en-echelon</i> tears, sag ponds/ swamps. | Rupture occurs across relatively flat alluvial valleys and across small ridges. |
| Karadere | 35 | N80°E | right lateral | 1.5 1-1.5 | No data | No data | No data | | 1 or 2 primary splays, linear drainages, scarps. | Rupture occurs in part along base of steep mountain front and linear stream valleys. |

¹Gölcük and Sakarya segments include distinct normal fault subsegments at margins of fault stepovers.²Width of fault zone estimated from field reconnaissance and surveying of selected locations.

Table 2.2. Fault Stepover Characteristics, August 17, 1999, Kocaeli (Izmit) Earthquake Rupture

| Stepover | Fault Normal Width (km) | Fault Parallel Length (km) | Stepover Area (km ²) | Stepover Type ¹ | Description of Stepover |
|--------------|-------------------------|----------------------------|----------------------------------|----------------------------|--|
| Karamürsel | 4 to 5 | 16 to 19 | 80 to 95 | Right-stepping overlap | Bathymetry indicates rhomboid graben bounded on all sides by faults. Yalova segment borders northern margin; Gölcük segment borders southern margin. Western margin locally extends onshore, forming marsh and lagoon on Hersek Peninsula. August 17 earthquake produced subsidence of basin, including localized subsidence of marsh on Hersek Peninsula. Basin arrested up to 5.5 meters of right slip on Gölcük segment. |
| Gölcük | 1 to 2 | 6 | 6 to 12 | Right-stepping separation | Basin formed by right separation between Gölcük segment and Sapanca segment. Bathymetry suggests asymmetric down-to-southwest graben. No prominent fault borders northern margin of graben. Fault segments are connected by prominent northwest-trending normal-oblique faults. August 17 earthquake broke through the basin producing normal faulting and global subsidence, including subsidence of part of the city of Gölcük. |
| Lake Sapanca | 1 to 2 | 7 | 7 to 14 | Right-stepping | Basin formed by right separation or overlapping stepover between Sapanca segment and Sakarya segment. Basin also occurs at right-releasing bend and stepover to the Mudurnu branch of the NAF. Basin is long and narrow. Bathymetry suggests that the basin is bordered on the north by the Sapanca fault segment and on the south by diffuse normal faulting. The Sakarya segment does not appear to extend offshore into Lake Sapanca along the southern margin of the basin. August 17 earthquake broke through the basin, producing normal faulting and localized subsidence and lateral spreading within the basin. |

Table 2-2 continued on next page

Table 2.2. *Continued* Fault Stepover Characteristics, August 17, 1999, Kocaeli (Izmit) Earthquake Rupture

| Stepover | Fault Normal Width (km) | Fault Parallel Length (km) | Stepover Area (km ²) | Stepover Type ¹ | Description of Stepover |
|------------|-------------------------|----------------------------|----------------------------------|---|--|
| Akyazi | 1 to 2 | 6 to 13 | 6 to 26 (18 to 20 preferred) | Left-stepping separation and 19° restraining bend | The Akyazi gap forms at the intersection of the west-trending Sakarya segment and east-northeast-trending Karadere segment. During the August 17 earthquake, right slip progressively decreased and died out on both sides of the gap as a series of left-stepping <i>en echelon</i> faults. Rupture gap coincides with Akyazi/Mudurnu River plain. Surface expression of fault rupture may have been masked or attenuated by unconsolidated deposits in the area. |
| Eften Lake | 2 to 4 | 9 | 18 to 36 | Double right-stepping separation | Basin appears to be a double right separation between the Karadere segment and Düzce segment, with a short (6 to 8 km long) intervening fault segment. Each stepover is about 2 km wide for a total basin width of about 4 km. The basin arrested both the August 17 rupture (1 to 1.5 meters on the Karadere segment) and the November 12 rupture (4 to 4.5 meters on the Düzce segment). Both earthquakes ruptured all or parts of the intervening 6- to 8-km-long segment within the basin, producing minor right slip displacements of 5 to 30 cm. The November 12 earthquake produced extensive normal-oblique faulting on northwest-trending faults in the eastern part of the double basin. |

¹After definitions of stepover type by Barka and Kadinsky-Cade (1988).

On the Düzce segment, minor right-lateral displacements of up to 20 cm were observed along the westernmost 2 to 3 km of the fault (USGS 2000). It appears likely that rupture of the Karadere segment during the August 17 earthquake locally stressed the adjoining Düzce segment, producing sympathetic displacement. This segment subsequently ruptured during the November 12 M_w 7.1 earthquake, producing up to 4.5 meters of displacement.

The Yalova segment crosses the Hersek and Yalova Peninsulas in Izmit Bay (plate 1). On the Hersek Peninsula, no significant ground rupture was observed, although minor ground cracking with a few centimeters of lateral displacement did occur locally over a broad zone of several hundred meters in the town of Hersek. In addition, minor surface rupture occurred along a linear trend crossing the Yalova Peninsula. In this area, extensional cracking and normal displacements of up to 30 cm occurred with minor right-lateral displacements of a few centimeters along continuous cracks in a delta fan. The ground rupture near Yalova may be the result of a large, deep-seated lateral spread. However, the length of the feature and the existence locally of what appears to be a pre-existing scarp suggest that the ground rupture is related to slight movements on the Yalova fault segment. It also is possible that minor displacements along the Yalova segment are related to aftershock activity.

Aftershock data, SAR interferometry data, and GPS data also suggest that minor rupture (<1 meter) may have occurred along the Yalova fault segment west of the Gölcük segment. Aftershock data for the first month following the August 17 earthquake show a distinct cluster of seismicity west of the city of Yalova and minor but distinct activity in western Izmit Bay (figure 2.3). Although significant surface rupture was not observed on the Hersek or Yalova Peninsulas, most of the Yalova segment lies offshore in western Izmit Bay. Aftershock and GPS data suggest that rupture may have extended an additional 40 to 70 km to the west of the Hersek Peninsula. If so, the total fault rupture would be approximately 170 to 200 km long. Alternatively, minor faulting on the Yalova segment may be sympathetic displacement similar to that which occurred on the Düzce segment following the August 17 earthquake. If so, this may suggest that the Yalova segment has been stressed to near the rupture threshold.

In our opinion, the minor displacement observed on the Düzce fault segment to the east and the Yalova fault segment to the west most likely represent secondary sympathetic displacements. These displacements probably did not contribute significantly to seismic moment release during the earthquake. The estimated total rupture length of 126 km for the August 17 earthquake, therefore, does not include the observed minor displacements on the Düzce and Yalova fault segments.

RUPTURE MORPHOLOGY

For most of the August 17, 1999, Kocaeli earthquake rupture length, the fault lies north of the steep range front of the Naldöken, Kapiorman, and Almacik Mountains (plate 1). Fault rupture generally occurred across the floors or edges of alluvial basins and only locally followed the prominent mountain range front to the south of the rupture zone. In many places, fault rupture occurred along a previously mapped fault trace characterized by geomorphic features such as degraded scarps, shutter ridges, pressure ridges, linear drainages, sag ponds, and tectonic depressions. In particular, rupture along the Karadere, Sakarya, and Sapanca segments commonly followed pre-existing topographic breaks at the base of low hills and locally followed contacts and erosional scarps between Holocene valley alluvium and slightly elevated older alluvium (Pleistocene lake and alluvial fans; figure 2.1). The eastern part of the Karadere segment generally trends along, or directly north of, the Almacik Mountain range front. This section of the fault curves

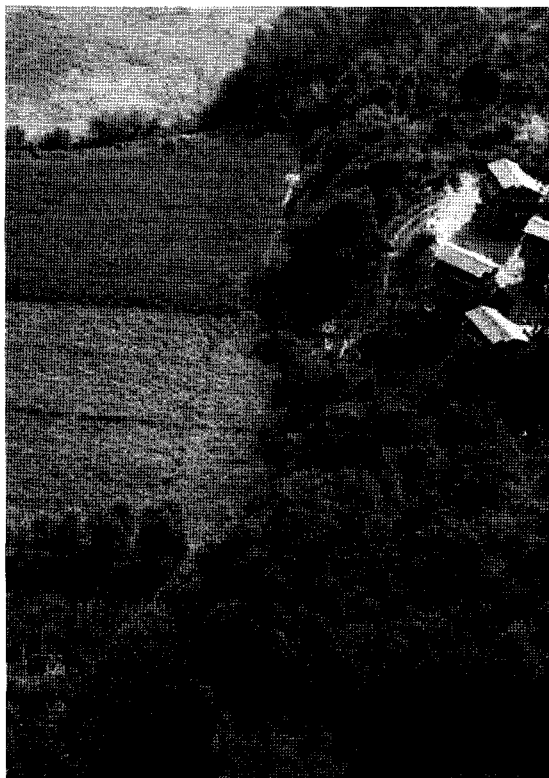


Figure 2.1. *Left* Fault rupture extends along eroded scarp between Holocene valley alluvium and elevated Pleistocene alluvium.

Figure 2.2. *Above* Moletrack along Sapanca segment produced by 3.1 meters of right lateral-offset.

northward around a bend in the fault zone, to run in a more northerly direction than the other fault rupture segments (plate 1). At its easternmost end, the Karadere segment followed straight stream segments, commonly diverging from the range front across slopes and side-hill benches.

In other areas, the rupture diverged from mapped bedrock fault traces or hill fronts and extended across relatively level alluvial plains that show no, or little, evidence of past rupture events. The primarily strike-slip nature of the rupture typically formed low moletracks across flat alluvial plains (figure 2.2). Geomorphic features of this nature commonly are destroyed quickly by erosion and grading. Along most of the Sakarya and Sapanca segments, the fault trace cuts across alluvial valleys, plains, and distal portions of alluvial fans between Akyazi and Izmit. The rupture between the Sakarya and Sapanca segments extended into the Lake Sapanca extensional stepover basin and is under water. Most of the Gölcük segment is located offshore in Izmit Bay, where it forms the relatively linear coastline, with the notable exception of a 2-km section that extends onshore at the Gölcük Naval Base and exhibited a maximum displacement of 5.5 meters (figure 2.3). Locally, the Gölcük rupture closely follows the base of a pre-existing linear pressure ridge on the naval base.

RUPTURE WIDTH

Fault rupture varied in width from a simple narrow zone of primary deformation a few meters wide, with little or no secondary deformation, to a broad zone of primary and secondary deformation up to 200 meters wide. Generally, the fault rupture consisted of one or two primary traces within a zone of distributed secondary deformation. The primary traces typically were

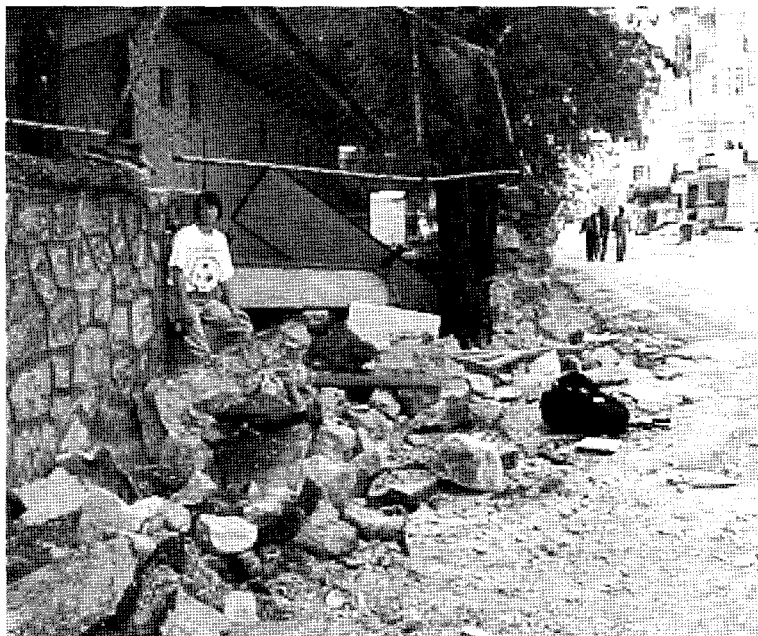


Figure 2.3. Right-lateral fault offset of stone wall along western margin of Gölcük Naval Base. Total fault offset at time of photo (September 2) was 4.2 meters. Subsequent measurement of the offset on October 2 showed cumulative offset of up to 5.5 meters.



Figure 2.4. Left-stepping *en-echelon* steps in the surface rupture along the Sapanca segment.

separated by 5 to 20 meters and commonly exhibited a left-stepping *en echelon* pattern at scales ranging from a few meters to several hundred meters (figure 2.4). Surveys of offset fence lines, roads, and tree lines show that the primary fault traces typically accommodated 80 to 90% of the fault displacement, with the remaining deformation distributed over a zone generally 20 to 50 meters wide.

The width of deformation appears to be controlled primarily by local fault geometry and rupture mechanics. Where the fault trace deviated in orientation from the prevailing strike of the fault, rupture complexity and width of the zone of deformation increased. In these areas, the primary fault trace(s) generally accommodated 50 to 80% of the fault displacement, with the remaining deformation distributed over a zone up to 200 meters wide. In addition, where fault rupture approached the end of a fault segment and/or entered a pull-apart basin, rupture complexity and width of the zone of deformation increased. In these areas, the amount of lateral slip decreased abruptly over a short distance, and distributed right shear with localized normal displacement occurred over a zone up to 1 km wide. Fault rupture zone width typically was narrower where it followed pre-existing scarps or prominent breaks-in-slope. Conversely, other possible controls on the width of fault rupture, such as thickness, age, and depositional environment of surficial deposits, did not appear to significantly affect the width or complexity of surface deformation. However, a more systematic evaluation of the fault rupture relative to the distribution and thickness of surficial deposits should be performed before this preliminary observation can be confirmed. There are areas (e.g., Akyazi stepover) where the amount of surface displacement along the fault trace may have been attenuated, in part, by deep soil deposits.

AFTERSLIP

Several cases of afterslip were reported following the August 17 earthquake. The best example of afterslip occurred at the Gölcük Naval Base, where fault rupture offset a stone wall. On September 2, total offset of the wall was measured at 4.2 meters (figure 2.3). On October 2, total offset of the wall was measured at up to 5.5 meters. Multiple surveys at several other sites suggest that afterslip of a few tens of centimeters occurred on both the Sapanca and Gölcük fault segments. No observations were made along the Sakarya and Karadere fault segments to document the presence or absence of afterslip.

FAULT SEGMENTS AND PULL-APART BASINS

One of the more interesting aspects of the August 17, 1999, earthquake is that fault rupture involved four distinct segments of the NAF. Segment end points are defined by right-releasing stepovers or gaps in the fault trace. Distinct structural basins have formed within the right-releasing stepovers, indicating that these segmentation points are long-lived features in the displacement history of the fault. The rupture, therefore, provides excellent empirical data on the amount of coseismic displacement that can and cannot propagate through fault stepovers of different dimensions.

Fault segments involved in the earthquake include, from west to east, the Gölcük, Sapanca, Sakarya, and Karadere segments (plate 1). Rupture characteristics for each of these segments are provided in table 2.1. Of note, each of the segments had different maximum and average amounts of surface displacement. In particular, the Karadere segment produced surface displacement of only 1 to 1.5 meters, generally one third or less than the amount of surface displacement observed on the other three segments. The Karadere segment was the segment farthest from the earthquake epicenter (>65 km east). Based on the amount of surface rupture, the Karadere segment appears to be a distinctly different rupture event and may represent a distinct subevent in the August 17 earthquake sequence (Toksöz et al. 1999).

Each of the fault segments can be distinguished on the basis of physical and behavioral characteristics. The Gölcük segment lies primarily offshore in Izmit Bay and defines the straight coastline between Karamürsel and Gölcük. The offshore extent of rupture is interpreted on the basis of pre- and post-earthquake bathymetry and the extent of shoreline subsidence. To the west, the Gölcük segment forms a 5-km-wide right-releasing stepover to the Yalova fault segment across the Karamürsel pull-apart basin (figure 2.5a, b). To the east, the Gölcük segment forms a 1- to 2-km-wide right-releasing stepover to the Sapanca segment across the Gölcük pull-apart basin (figure 2.6a, b). The east end of the Gölcük fault dies out within the Gölcük pull-apart basin. The basin is bounded on the southwest by a prominent normal fault. Up to 2.4 meters of vertical offset occurred along the normal fault. The fault locally follows a pre-existing 2- to 6-meter-high scarp preserved in late Holocene deposits, suggesting that the fault has experienced several previous ruptures in the Holocene.

The Sapanca segment traverses broad, alluvial floodplains and bedrock ridges and is defined by well-expressed sag ponds (marshes), linear drainages, side-hill scarps, and tonal lineaments. To the east, the Sapanca segment forms a 1-km-wide right-releasing stepover to the Sakarya segment across the Sapanca pull-apart basin (figures 2.7a, b). In addition, the Sapanca basin forms the intersection of the August 17 fault rupture with the southern branch of the NAF, which most recently ruptured during the 1967 M_w 7.0 Mudurnu Valley earthquake (plate 1).

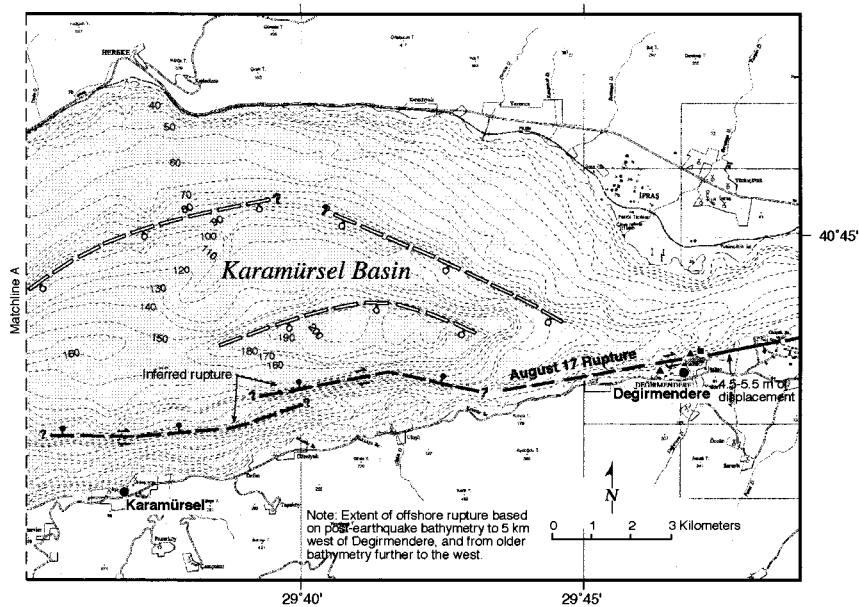
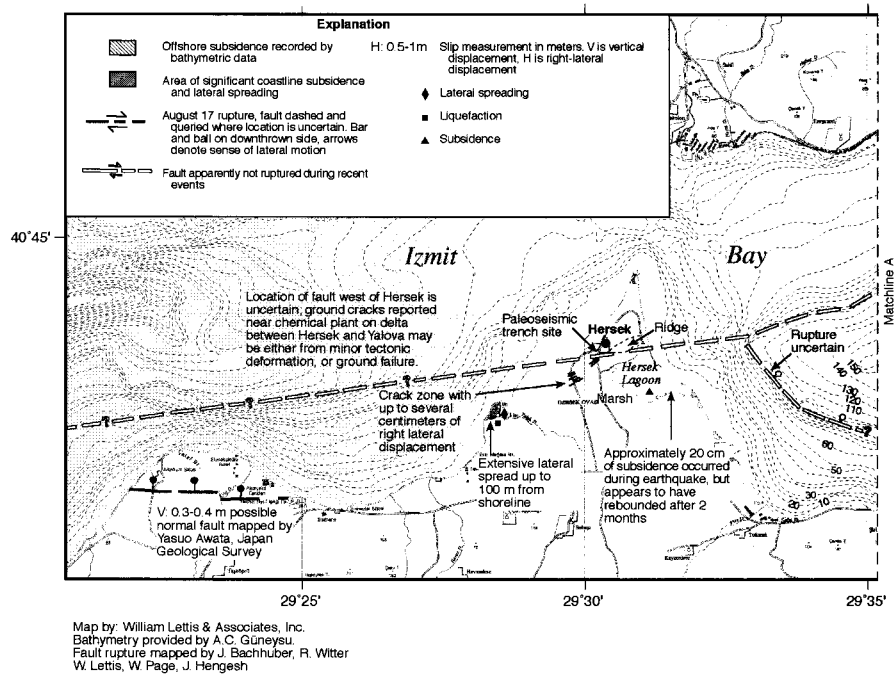
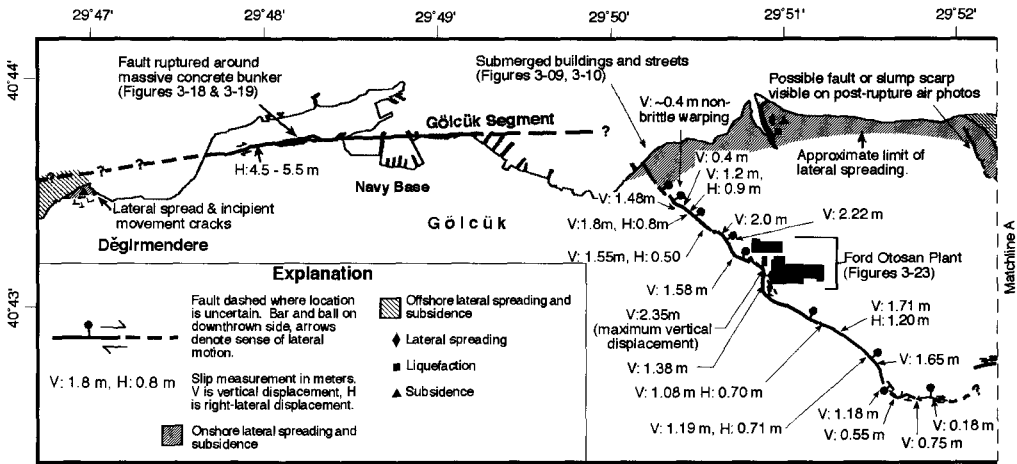


Figure 2.5a, b. Karamürsel stepover basin and western extent of rupture along the Gölçük fault segment.



Map by: William Lettis & Associates, Inc.
Normal fault rupture mapped by E. Altunel, T. Dawson
Gölçük and Sapanca segments mapped by J. Bachhuber, W. Lettis,
W. Page, J. Hengesh, A. Kaya.

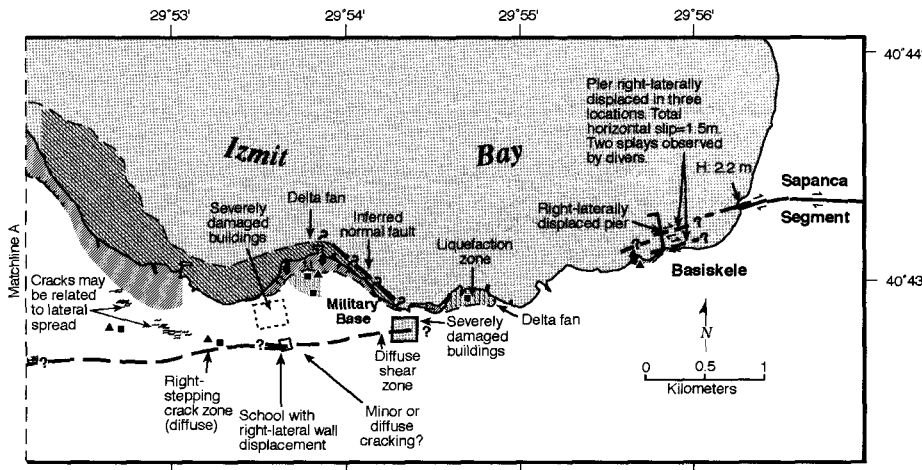
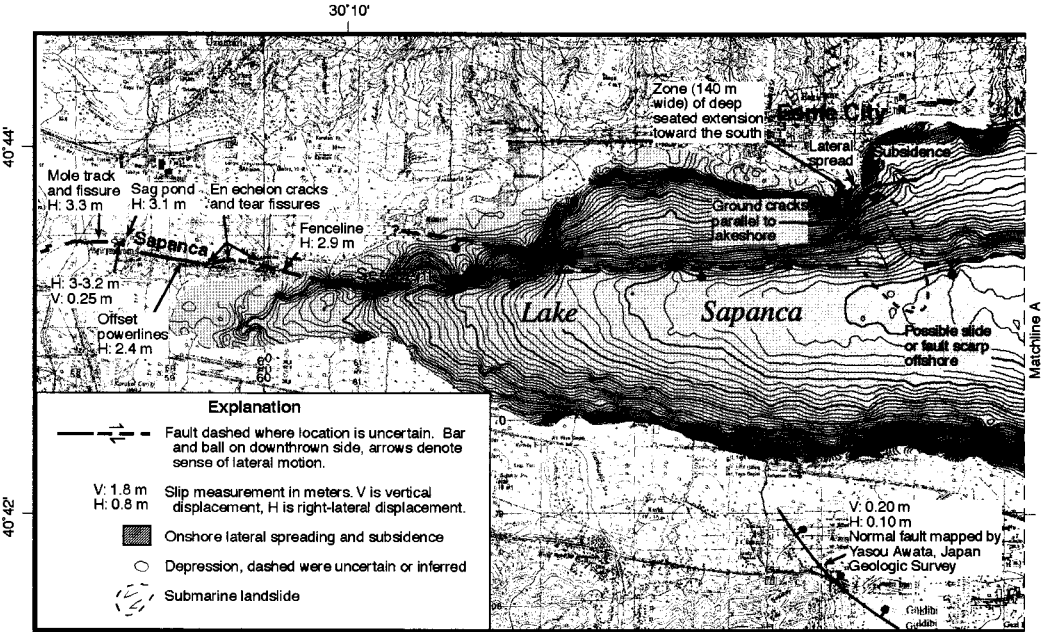


Figure 2.6a, b. Gölçük stepover basin and central and eastern part of Gölçük fault segments.



Map by: William Lettis & Associates, Inc.
Bathymetry provided by: A. Kaya, funding provided by
Pacific Gas & Electric Company and
Pacific Earthquake Engineering Center.
Fault rupture mapped by J. Bachhuber, J. Hengesh, W. Lettis & W. Page.

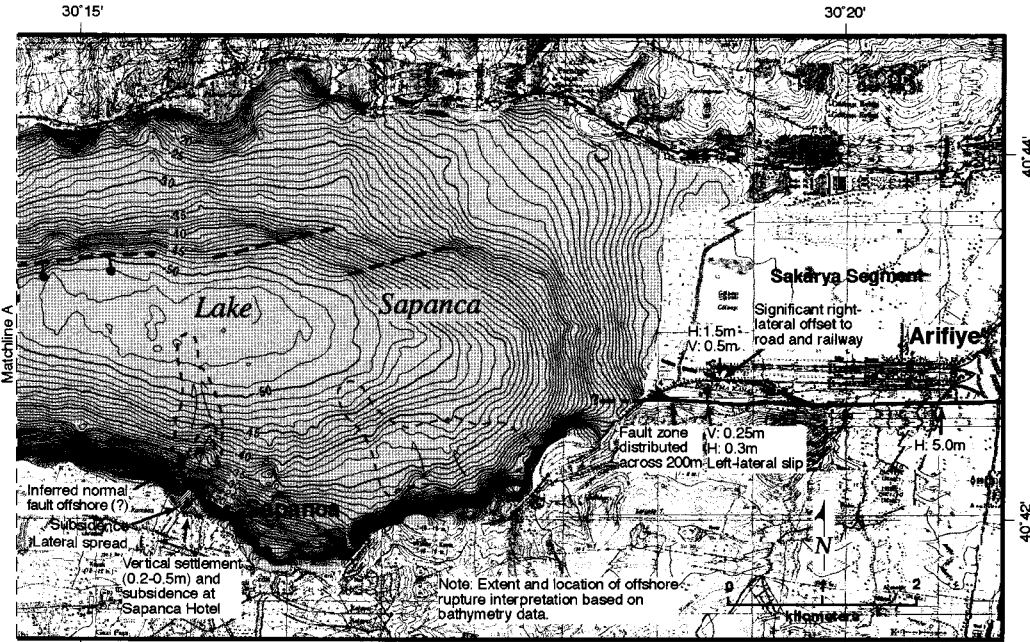


Figure 2.7a, b. Lake Sapanca stepover basin and portions of the Sapanca and Sakarya fault segments.

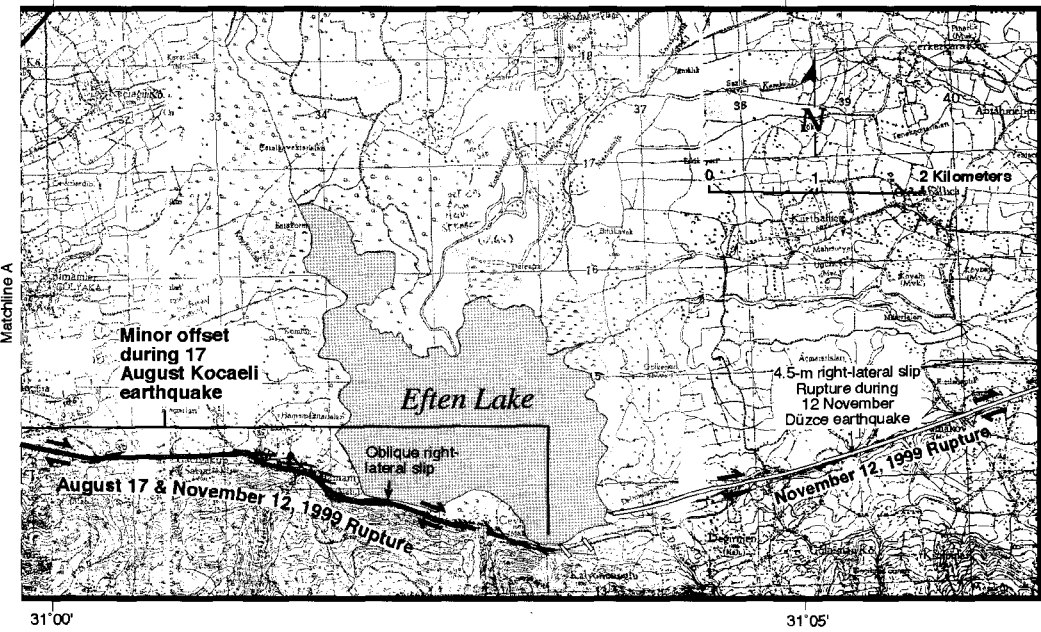
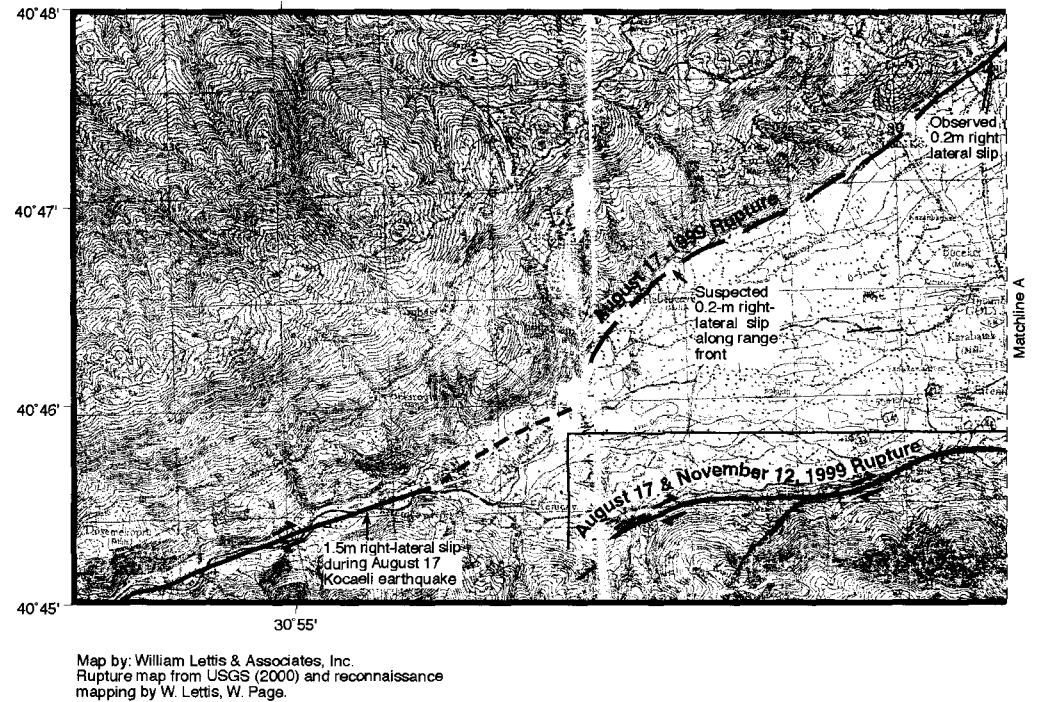


Figure 2.8a, b. Eften Lake right-stepping double pull-apart at eastern termination of the August 17, 1999, Kocaeli earthquake rupture. A small fault at the southern margin of the basin experienced slight displacement during the Kocaeli and November 12, 1999, Düzce earthquakes. The Düzce earthquake initiated in or near the Eften Lake pull-apart, and ruptured eastward along the Düzce fault.

The Sakarya segment traverses a broad alluvial valley and is well expressed by sag ponds, linear scarps and pressure ridges, and tonal lineaments. To the east, the Sakarya segment dies out in a series of left-stepping *en echelon* fault traces within the Akyazi basin. Slip on the segment abruptly decreases to between 0.5 and 1 meter. The Sakarya segment is separated from the Karadere segment by a 1- to 2-km-wide, 6-km-long left-restraining gap in the fault trace (plate 1).

The Karadere segment trends about 19° more northerly than the Sakarya segment and lies at or near the base of a steep range front. It is defined by linear drainages, fault scarps, and tonal lineaments. To the east, the segment forms a 4- to 6-km-wide double right-releasing stepover to the Düzce segment across the Eften Lake pull-apart basin (figure 2.8a, b).

KARAMÜRSEL PULL-APART BASIN

The Karamürsel basin is about 5 km wide and 16 to 19 km long (table 2.2, figure 2.5a, b). Based on interpretation of bathymetric data, the basin is formed by a right-stepping overlap of the Yalova and Gölcük fault segments. The basin area is about 80 to 95 km². The basin appears to have arrested up to 5.5 meters of westward propagating right-lateral displacement on the Gölcük segment (observed on the Gölcük Naval Base). Displacement along the Gölcük segment extending offshore along the southern margin of the Karamürsel basin is inferred, based on the presence of extensive lateral spreading and offshore subsidence at various locations along the coastline, in particular near the towns of Degirmendere (chapter 4, figure 4.9) and Halidere.

Field reconnaissance on the Hersek Peninsula clearly shows that significant fault rupture did not extend onshore along the trend of the Gölcük segment or along the Yalova segment bordering the northern margin of the Karamürsel basin (figures 2.5a, b). There was no evidence of significant rupture along mapped older fault traces at the mountain front south of the Hersek Peninsula on trend with a westward projection of the Gölcük fault segment. On the Hersek Peninsula, the Yalova fault segment is geomorphically well expressed by linear depressions, a sag pond, a linear ridge, tonal lineaments, and truncated or offset late Pleistocene beach ridges. The geometry and location of the Hersek Lagoon is consistent with westward growth of the Karamürsel pull-apart basin and encroachment onto the Hersek Peninsula. Paleoseismic trenches excavated during our reconnaissance mapping across the north margin of the Hersek Lagoon documents the presence of the Yalova fault and the absence of rupture during the August 17 earthquake. No ground rupture was observed in the area following the earthquake, although Hersek Lagoon reportedly subsided by about 20 to 30 cm.

GÖLCÜK PULL-APART BASIN

The August 17 earthquake appears to have nucleated within the Gölcük pull-apart basin. The earthquake epicenter generally plots within or directly north of the basin (plate 1). Rupture propagated bilaterally to the west along the Gölcük fault segment and to the east along the Sapanca, Sakarya, and Karadere fault segments (Pinar et al. 1999). Right slip of 4.5 to 5.5 meters occurred on the Gölcük segment at the western end of the basin, and 3 meters occurred on the Sapanca segment at the eastern end of the basin. Slip on the Sapanca segment progressively decreased into and along the southern margin of the Gölcük pull-apart basin, producing minor ground cracking directly east of Gölcük (figures 2.6a and 2.6b).

The earthquake also produced significant tectonic subsidence within the basin. Vertical displacement of up to 2.4 meters occurred on a continuous normal fault along the southwestern margin of the basin (figures 2.6a, b). Additional down-to-the-east normal faulting appears to have occurred along the coast directly east of Gölcük. The normal faulting produced global subsidence of the basin and locally caused submergence of the coastline and widespread inundation of the

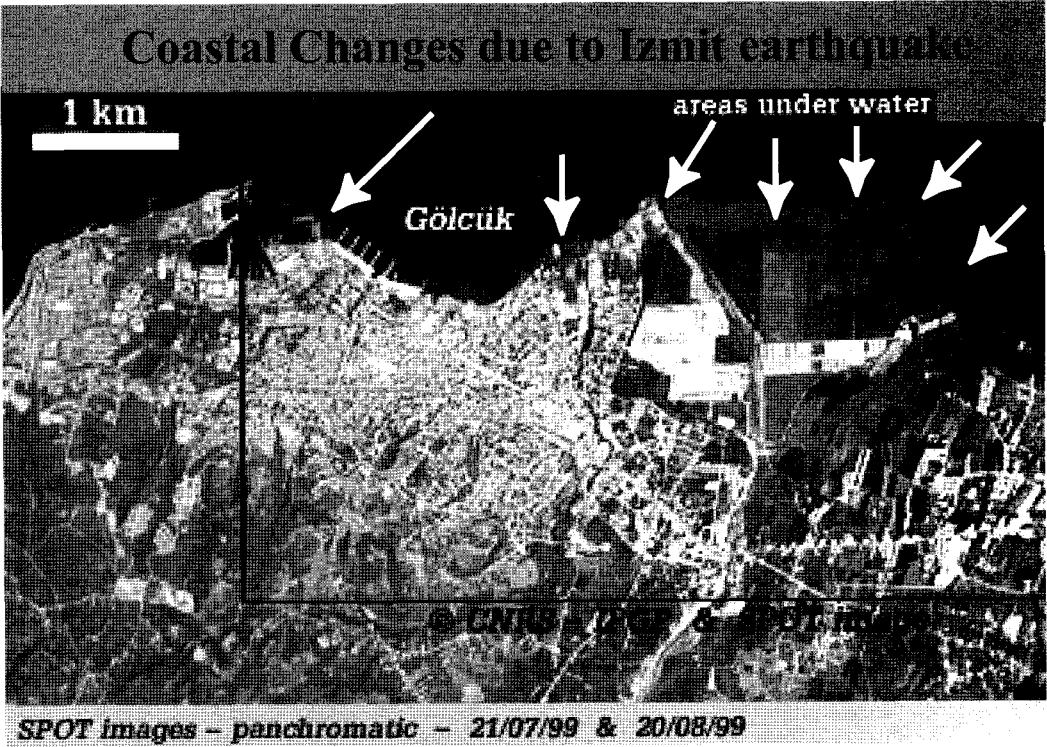


Figure 2.9. SPOT satellite image with enhanced blue shading delineating areas of flooding and subsidence within a tectonically down-dropped block along the south margin of Izmit Bay at Gölcük.

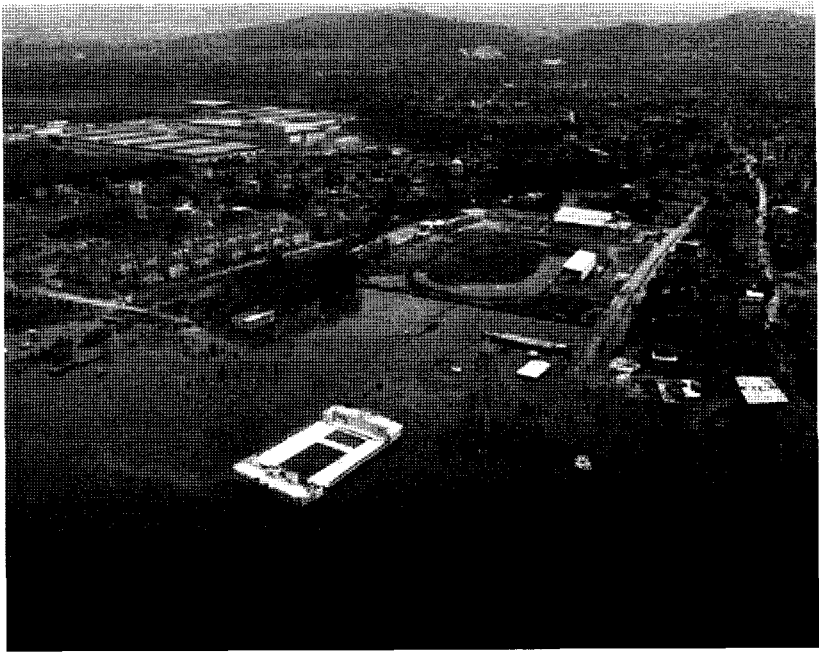


Figure 2.10. Widespread tectonic subsidence in eastern Gölcük City caused by normal faulting and subsidence of the Gölcük pull-apart basin.

northeastern part of Gölcük city (figures 2.9, 2.10). Evaluation of pre- and post-earthquake bathymetry shows that several near-shore areas also subsided from 2 to 6 meters (plate 1, figure 2.6).

The Gölcük basin is about 1 to 2 km wide and up to 6 km long (table 2.2, figure 2.6a, b). The basin is formed by a right stepover or right separation between the Gölcük and Sapanca segments. Based on interpretation of bathymetric data, the Gölcük segment may or may not extend along the northern margin of the basin; thus, we cannot determine the amount of overlap, if any, between the two fault segments. The basin area is about 6 to 12 km².

SAPANCA PULL-APART BASIN

The Sapanca basin is about 1 to 2 km wide and up to 7 km long (table 2.2, figure 2.7a, b). Based on interpretation of bathymetric data, the basin is formed by a right stepover or separation between the Sapanca and Sakarya fault segments. The Sapanca fault segment defines the northern margin of the basin and extends almost entirely across Lake Sapanca to the eastern margin of the lake. The fault is expressed by a prominent scarp on the floor of Lake Sapanca. The Sakarya segment appears to die out at the eastern margin of the basin and is not expressed by bathymetry in Lake Sapanca. Rather, the southern margin of the Sapanca basin appears to be defined by a series of northwest-trending normal faults. In addition, the Mudurnu Valley segment of the southern branch of the NAF intersects the Sapanca segment at Lake Sapanca (plate 1). This intersection forms a larger 5-km-wide stepover and right-releasing bend in the southern branch of the NAF. Rupture during the M_w7.0 Mudurnu Valley earthquake of July 22, 1967, was arrested by this larger stepover at Lake Sapanca. Reported ground fissures observed near Sapanca and Esme following the 1967 Mudurnu Valley earthquake (Berg 1967) are considered to be related to large-scale lateral spread or liquefaction rather than primary tectonic rupture. Similar continuous cracks developed in these areas from lateral spread failure during the August 17 earthquake. Hence, surface fault rupture from the 1967 Mudurnu Valley earthquake is shown to terminate southeast of Sapanca on plate 1.

Rupture during the earthquake broke through the Sapanca stepover between the Sapanca and Sakarya fault segments. About 3 meters of right slip was observed on both the Sapanca and Sakarya segments near the lake. Right slip began to die out within 1 km of the shoreline as each fault entered the basin. In particular, right slip decreased from 3.5 meters to about 1 meter on the Sakarya segment near the eastern margin of Lake Sapanca (figures 2.7a, b). The pull-apart basin area is about 7 to 14 km². The earthquake also produced normal offset of about 30 cm on one normal fault south of the pull-apart basin, southwest of the town of Sapanca (Y. Awata, personal communication, 1999). Extensive subsidence also occurred along the southern coast of Lake Sapanca near the town of Sapanca. A notable occurrence of liquefaction and lateral spreading occurred near Hotel Sapanca, as described in chapter 6. An offshore scarp 2 to 3 meters high near the hotel may be the margin of a lateral spread or, equally likely, may be displacement on a normal fault along the lake margin.

AKYAZI STEPOVER

The Akyazi stepover is a 1- to 2-km-wide left-stepping separation between the Sakarya fault segment and the Karadere fault segment (plate 1). The Karadere segment also trends 19° more northerly than the east-west-trending Sakarya segment, forming a left-restraining bend in the fault zone.

Rupture during the earthquake broke through the Akyazi stepover and left-restraining bend. Approximately 3 meters of right slip on the Sakarya segment progressively died out into the Akyazi stepover as a series of left-stepping *en echelon* fault traces. After approximately a 6- to 8-km-long gap in the rupture, right slip progressively increased to 1 to 1.5 meters on the Karadere segment. The rupture gap coincides with the Akyazi/Mudurnu alluvial plain. Surface expression of fault rupture may have been masked or attenuated, in part, by unconsolidated deposits in the area.

The length of the Akyazi stepover is estimated to be 6 to 13 km. Six kilometers is the minimum length of the rupture gap between the Sakarya and Karadere segments and includes the 19° restraining bend in the fault zone. Thirteen kilometers includes the easternmost 7 km of the Sakarya segment, where right slip decreased significantly and broke up into a series of left-stepping *en echelon* fault traces. Total area of the restraining stepover, therefore, is 6 to 26 km², with a preferred value of about 18 to 20 km².

EFTEN LAKE STEPOVER

The Eften Lake stepover appears to be a double-releasing stepover between the Karadere fault segment and the Düzce fault segment, with a short (6 to 8 km long) intervening fault segment (figure 2.8a, b). Each stepover is about 2 km wide, for a total stepover width of about 4 km. The total stepover length is about 9 km, indicating a stepover area of about 18 to 36 km².

The Eften Lake stepover arrested rupture during both the August 17 and November 12 earthquakes. Rupture of 1 to 1.5 meters occurred on the Karadere segment during the August 17 earthquake. This rupture progressively died out into the stepover basin, producing minor (up to 20 cm) right slip both on the intervening 6- to 8-km-long fault segment (USGS 2000) and along the southeast-facing rangefront bordering the northwestern margin of the basin (figure 2.8a, b).

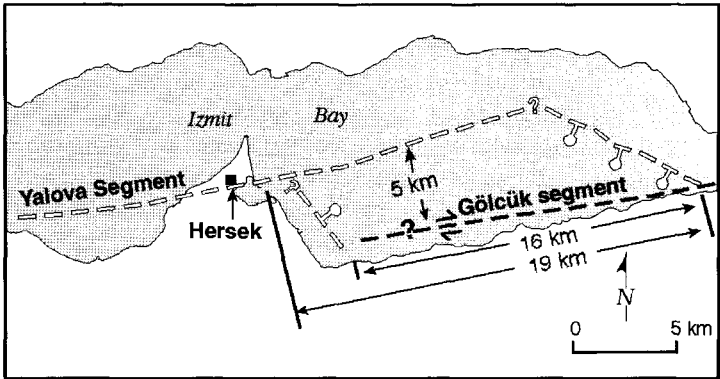
The November 12 earthquake nucleated within or near the eastern margin of the stepover and produced unilateral east-propagating right-slip rupture of 4 to 4.5 meters on the Düzce segment. The earthquake also produced significant vertical slip of up to 4 meters along the southern margin of the basin. Slip occurred on an apparent normal fault connecting the Düzce fault with the intervening 6- to 8-km-long fault segment. Minor right-lateral slip of 20 to 30 cm also occurred on the intervening fault segment; thus, the intervening fault segment experienced minor rupture during both the August 17 and November 12 earthquakes.

PULL-APART BASIN COMPARISON

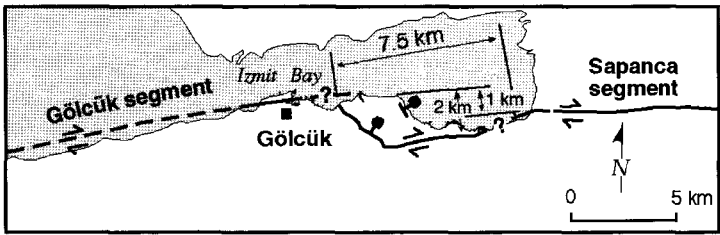
Four pull-apart basins were involved in the August 17 earthquake. These basins are shown at the same scale in figure 2.11 for comparison. The basins significantly influenced the distribution and length of fault rupture and, thus, provided broad controls on the size of earthquake magnitude. The Karamürsel stepover, a right-stepping overlap with a basin area of about 95 km², arrested up to 5.5 meters of rupture. The earthquake appears to have nucleated within the Gölcük pull-apart basin, producing bilateral rupture to the east and west. The stepover is a right-releasing separation between fault traces with a basin area of about 6 to 12 km². The Sapanca stepover is a right stepover with little or no fault overlap or separation. Fault rupture of about 3 meters broke through the basin. The basin area is about 7 to 14 km². The Eften Lake stepover is a double releasing right stepover with little or no fault overlap. The basin area is about 18 to 20 km². The basin arrested 1 to 1.5 meters of right slip during the earthquake. The November 12 earthquake appears to have nucleated within or near the basin, producing unilateral east-propagating rupture away from the basin.

THEORETICAL MODELING OF PULL-APART RUPTURE DYNAMICS

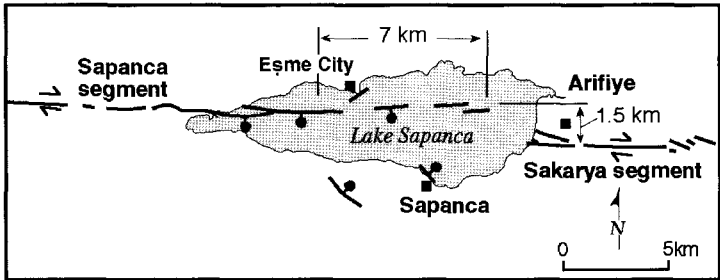
The distinctive segmented nature of the fault rupture during the August 17 earthquake provides an opportunity to investigate the influence of stepover size and geometry on the propagation of fault rupture. The relationship between strike-slip fault segmentation and fault rupture dynamics has been explored extensively by previous workers, with field examples (e.g., Aydin and Nur 1982; Barka and Kadinsky-Cade 1988), physical analog models (e.g., Dooley and McClay 1997; Reches 1987), and numerical models (Harris and Day 1993; Segall and Pollard 1980). The earthquake provides a wealth of high-quality field data on a single fault rupture event, including the fault trace, slip distribution, segment lengths, and stepover geometries. These data have been incorporated into



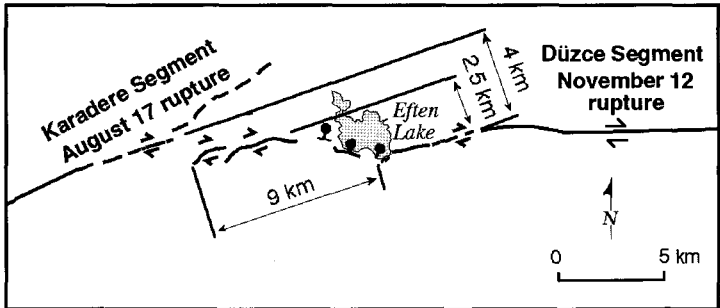
A. Karamürsel Stepi-over



B. Gölcük Stepi-over



C. Lake Sapanca Stepi-over



D. Eften Lake Stepi-over

Figure 2.11. Comparison of pull-apart basins along the August 17, 1999, Kocaeli earthquake rupture.

a simple numerical model to investigate the relationship between segmentation and surface rupture. The model utilizes Poly3D (Thomas 1993), a three-dimensional boundary element program that solves for stresses and displacements at points in a homogeneous, isotropic linear elastic half-space in the vicinity of faults.

Preliminary modeling illustrates the fault stepover geometries that are most favorable for continued fault rupture and which others tend to inhibit fault rupture. Analysis focused on two pull-apart basins in the region of the August 17 rupture: the Sapanca stepover basin and the Karamürsel stepover basin. These basins were chosen as endmember cases; the Sapanca pull-apart did not arrest fault rupture, while the Karamürsel stepover did appear to halt the rupture. Preliminary results suggest that the stress perturbation associated with up to 3 meters of slip along the Sapanca segment was sufficient to increase stress on the adjacent Sakarya segment and allow rupture to propagate eastward across the intervening pull-apart basin (figure 2.12). In addition, the model of the Karamürsel stepover indicates that the observed 4 to 5 meters of slip on the Gölcük segment did not appear to stress the Yalova segment enough to cause rupture. The preliminary results of the model suggest that fault stepovers with widths greater than 4 to 5 km can arrest up to 5 meters of fault rupture propagation, but that 3 meters of rupture can propagate across a 1- to 2-km-wide stepover. This model agrees with the field observations that the 5-km-wide Karamürsel stepover terminated further westward rupture of the Kocaeli earthquake.

EFFECTS OF SURFACE FAULT RUPTURE ON ENGINEERED STRUCTURES, FACILITIES, AND LIFELINES

Surface rupture from the August 17 earthquake caused extensive damage to engineered structures and lifelines. In a few instances, massive concrete structures and/or foundations influenced the surface expression of the fault rupture. Fault rupture traversed both rural and urban areas, providing excellent examples of the effects of surface rupture on buildings. In particular, fault rupture extended through the eastern part of Gölcük (figures 2.13, 2.14), the Gölcük Naval Base, the towns of Kullar and Arifiye, and numerous rural communities.

Surface rupture during the earthquake dramatically illustrated the damaging effects of surface fault rupture on structures, facilities, and lifelines. Although most of the damage during the earthquake resulted from strong ground shaking and permanent ground deformation due to liquefaction (Adapazari) and coastal landslides, surface fault rupture locally contributed significantly to the overall earthquake damage. Fault rupture contributed directly to the collapse of or significant damage to over a hundred buildings, fifty of which are located within or directly east of Gölcük. In addition, fault rupture severed many lifelines, including railroads, highways, and pipelines (water and sewer), contributing to significant delays in emergency response and loss of water and sewer service to many communities.

Fault rupture generally contributed to building damage where the primary trace of the fault passed directly beneath the structure. In many cases, where the fault rupture on the primary trace occurred within one meter of a building, the building was not damaged either by fault rupture or by strong ground shaking. In several instances, glassware, flowerpots, and other fragile items appear not to be disturbed in these apparently undamaged houses. However, in many other cases, buildings close to the fault were significantly damaged.

The following section provides photo-documentation of damage to structures caused by surface fault rupture. Documentation is provided from west to east along the fault trace, including examples from the Gölcük, Sapanca, and Sakarya fault segments.

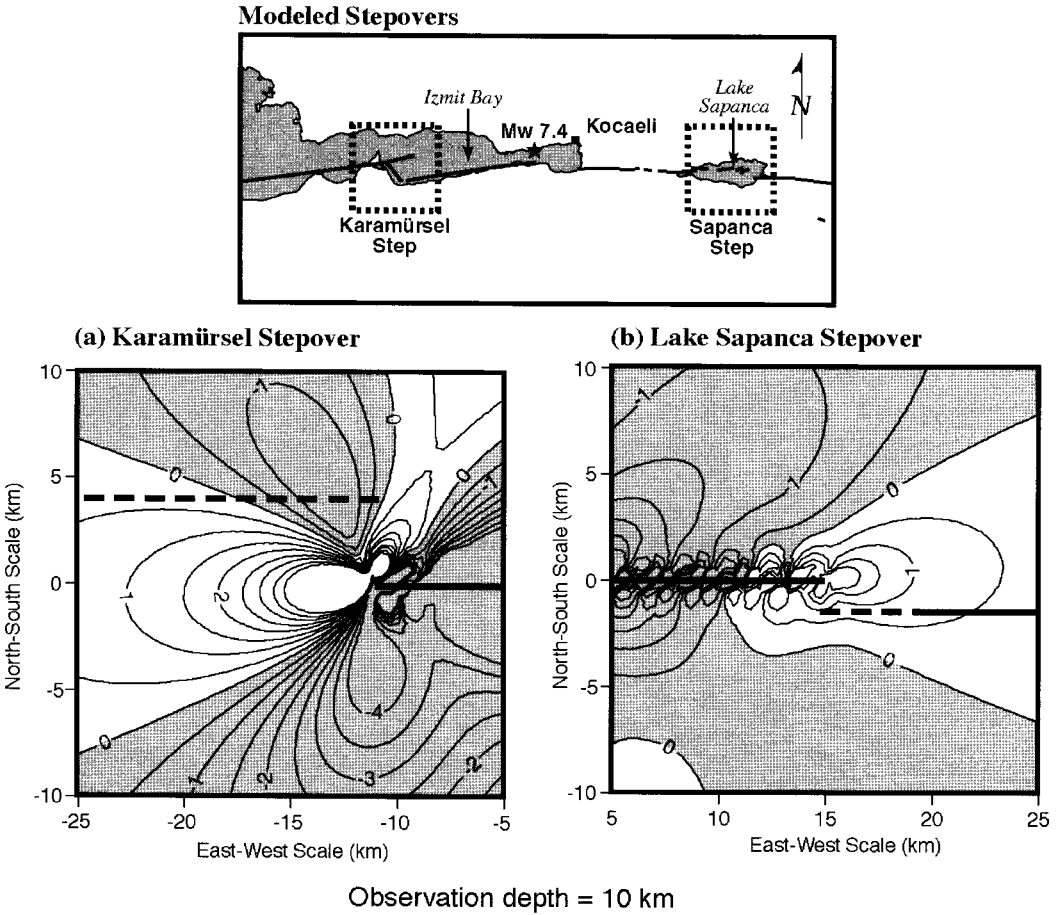


Figure 2.12. Model outputs for (a) Karamürsel and (b) Lake Sapanca fault steepers. (a) Contours of change in Coulomb stress (MPa) on east-west trending strike-slip faults caused by slip on the Gölcük fault segment. Approximate trace of the Yalova segment shown by dashed line. Fault rupture on the Gölcük segment was arrested at this steper and did not activate the Yalova segment. (b) Contours of change in Coulomb stress (MPa) on east-west trending strike-slip faults caused by slip on the Sapanca fault segment. Trace of the Sakarya segment shown by solid line, dashed where fault rupture is uncertain. Slip on Sapanca segment ruptured across this steper and continued onto Sakarya segment.



Figure 2.13. Aerial view of extensive damage in Gölcük with Izmit Bay in upper corner. Surface fault rupture extended through the city. Although most of the observed damage in this photo resulted from strong ground shaking, surface fault rupture contributed to damage when apartment buildings and houses lay astride the rupture.



Figure 2.14. Four-story apartment house that collapsed from surface rupture on right side of photo, west of Gölcük Naval Base. Fault rupture passes left to right across the middle of the photo between two standing apartment buildings. These apartment buildings were originally aligned and are now offset about 4 meters relative to one another across the fault.

EFFECTS OF SURFACE FAULT RUPTURE ON BUILDINGS AND STRUCTURES

Surface fault rupture caused complete collapse or significant damage to buildings directly astride the fault trace. In particular, significant damage occurred in the city of Gölcük along the Gölcük fault segment and from normal faulting related to subsidence of the Gölcük pull-apart basin (figure 2.10). Additional damage to buildings from fault rupture occurred in the town of Kullar along the Sapanca fault segment and the town of Arifiye on the Sakarya fault segment. Buildings also were damaged in rural areas where they were located on the fault rupture.

Gölcük Fault Segment

In the city of Gölcük, 4 to 5 meters of surface rupture occurred along the Gölcük fault segment (figures 2.6a and 2.6b). Several reinforced concrete frame apartment buildings collapsed or were heavily damaged by fault rupture in areas that were relatively undamaged by strong ground shaking (figure 2.14). Thus, fault rupture contributed directly to collapse of the buildings.

Surface fault rupture also damaged numerous buildings on the Gölcük Naval Base (figure 2.15). Fault rupture crossed the base near the southern margin of a linear pressure ridge and extended beneath a single-story building and a three-story building in the western part of the base (figures 2.16, 2.17). Both buildings were severely damaged by the rupture but did not collapse. Rupture also extended beneath a large officer quarters building on the base, causing complete collapse of the building and significant loss of life. A series of three buried bunkers are present



Figure 2.15. Aerial view of Gölcük Naval Base; view toward the south. Izmit Bay is in the foreground. The linear hill covered with trees in middle of photo is a pressure ridge along the Gölcük segment of the North Anatolian fault. Three to four meters of fault rupture occurred along the far side of the ridge, and extended through the naval base and docks.



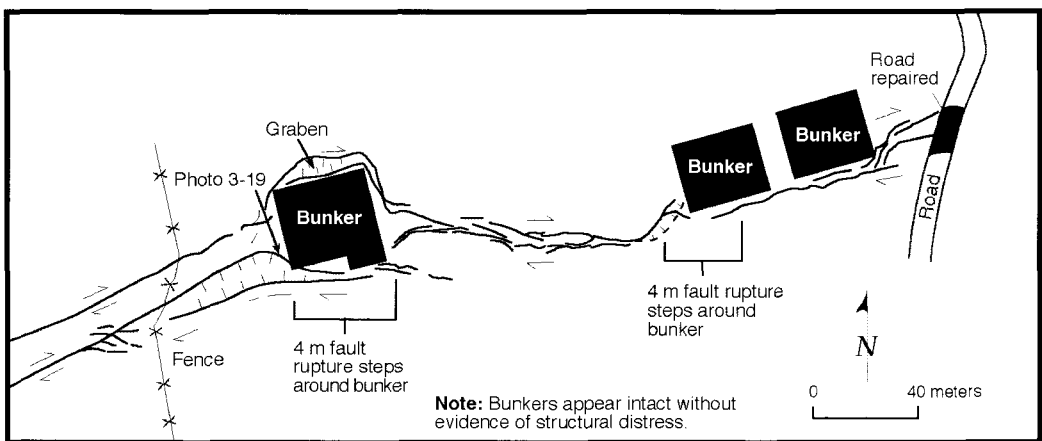
Figure 2.16. Fault rupture through single-story building, west part of Gölçük Naval Base.



Figure 2.17. Fault rupture between and through a complex of three-story buildings, west part of Gölçük Naval Base.

along the base of the linear pressure ridge. Fault rupture of 3 to 4 meters directly intersected the bunkers, which appear to be constructed of heavily reinforced concrete. The massive concrete bunkers caused the surface rupture to go around them (figure 2.18, 2.19). The bunkers did not appear to be damaged, although a small amount of counterclockwise rotation may have occurred.

Farther to the east on the Gölcük Naval Base, fault rupture extended offshore and crossed a series of docks and port facilities (figure 2.20). Displacement typically was transferred through the rigid structural members to weaker connections, joints, or elements of the docks or was accommodated by global rotation, thereby spreading the damage over a wider area (figure 2.21).



Mapped by: J. Bachhuber and W. Lettis

Figure 2.18. Surface rupture on Gölçük fault segment at Gölçük Naval Base broke around massive concrete bunkers without structural damage to the bunkers (see also figure 2.19).

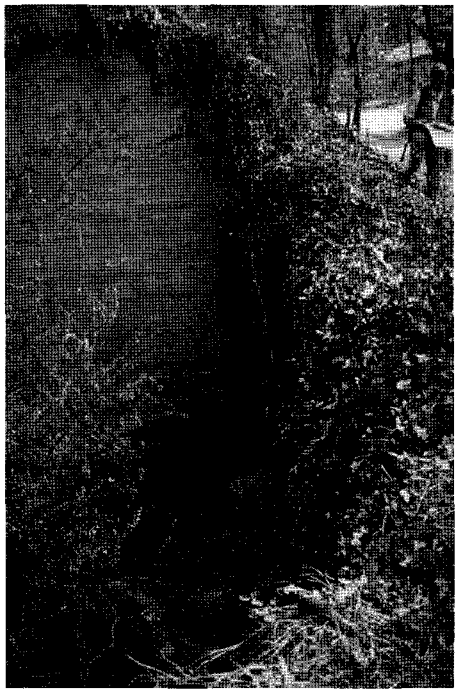


Figure 2.19. *Left* Fault rupture of 3 to 4 meters extending around undamaged bunker on south side of the pressure ridge (in figure 2.18), west part of Gölçük Naval Base. Rupture locally pulled the soil away from the bunker on one side, and compressed the soil on the other side.

Figure 2.20. *Above* Aerial view of the docks at Gölçük Naval Base. Surface faulting has displaced the docks, most clearly seen in the middle of the photo.



Figure 2.21. Fault offset of about 2 meters of a dock at the Gölcük Naval Base.

Gölcük Pull-Apart Basin

The Gölcük pull-apart basin is located in the right-releasing stepover between the Gölcük and Sapanca fault segments (plate 1, figures 2.6a and 2.6b). The eastern part of the city of Gölcük is located within the pull-apart basin. Fault rupture during the August 17 earthquake produced up to 2.4 meters of vertical displacement along a normal fault through the city and widespread tectonic subsidence within the basin. The vertical displacement and tectonic subsidence caused inundation of large parts of eastern Gölcük city (figures 2.9, 2.10). In eastern Gölcük city, several reinforced concrete frame structures with clay-tile infill walls located on the fault trace suffered partial to total collapse (figure 2.22). Many of these buildings collapsed in areas of widespread damage due to strong ground shaking; thus, the contribution of fault rupture to building damage is uncertain. At the Ford-Otosan plant, secondary fault rupture significantly damaged a large multicolumn truss assembly plant building (figure 2.23). Fault rupture of 30 to 40 cm extended below the southwest corner of the building. Differential distress to the building was transferred throughout the structure by truss displacement and tilting of the columns at the truss-column connections. This building is an excellent example of damage from secondary faulting.

Directly west of the Ford-Otosan plant, normal fault rupture extended beneath a large mosque (figure 2.24). Vertical displacement of approximately 1 meter caused collapse of the western part of the mosque.

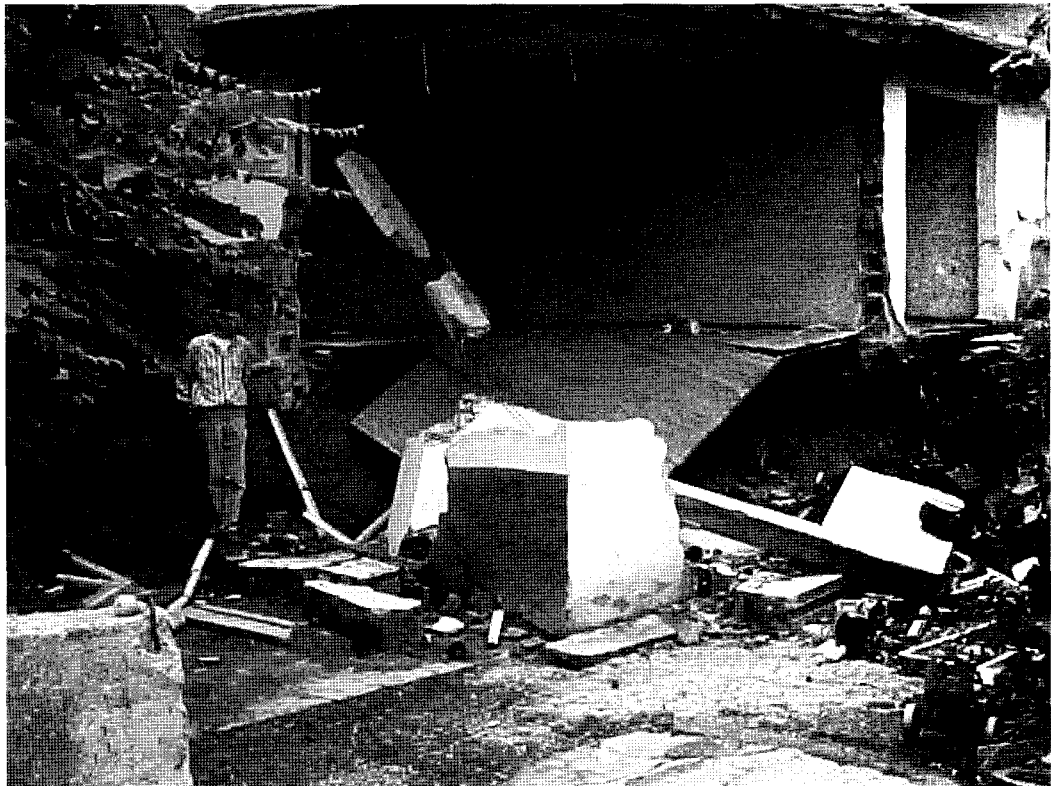


Figure 2.22. Concrete frame, clay-tile infill two-story apartment damaged by normal fault displacement of 1 to 2 meters in eastern Gölcük City.

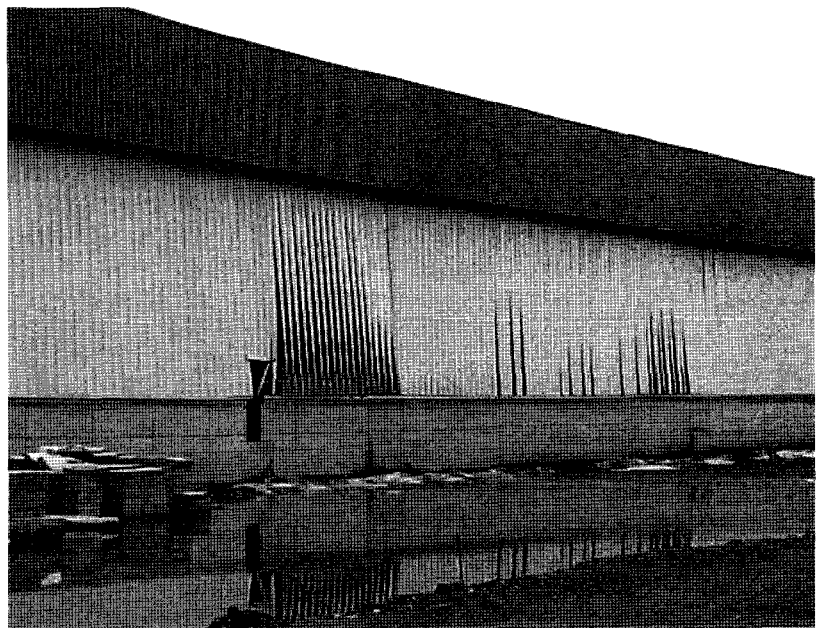


Figure 2.23. Wall of Ford-Otosan assembly plant building showing distress caused by secondary faulting beneath the building. Building consists of multi-column truss structure on a concrete slab. Secondary displacement of 30 to 40 cm significantly damaged the building.



Figure 2.24. Vertical surface displacement of about 1 meter extended beneath and caused collapse of a mosque in a residential area directly east of the city of Gölcük.

Sapanca Fault Segment

Approximately 3 meters of right-lateral displacement occurred on the Sapanca fault segment (plate 1). Fault rupture extended through the community of Kullar and residential areas nearby. For example, directly west of Kullar, 3.2 meters of lateral fault rupture extended beneath one of a group of seven six-story concrete frame apartment buildings (figure 2.25). All but one of the seven apartment buildings collapsed; thus, collapse of the apartments was due primarily to strong ground shaking and not fault rupture. In Kullar, surface rupture occurs on two primary fault traces. On one fault trace, 2 meters of lateral and 0.5 meter of vertical displacement caused partial collapse of the town's primary school (figure 2.26). Surrounding buildings were not significantly damaged by strong ground shaking; thus, collapse of the primary school was due to fault rupture. On the adjoining fault trace, about 1 meter of lateral displacement directly intersected a two-story building (figure 2.27). Displacement on the fault stopped at the building, and slip was transferred to the adjoining, subparallel fault trace. In eastern Kullar, 1 to 1.5 meters of fault rupture intersected a concrete frame four-story house under construction (figure 2.28). Rupture extended beneath the shallow foundation of the house but did not damage the foundation or concrete frame of the house.

Farther to the east, near Lake Sapanca, fault rupture occurs along the crest of a linear, east-west-trending ridge. About 1 km west of Lake Sapanca, the fault rupture directly intersects a Koran school building (figures 2.29, 2.30). About 1 to 2 meters of distributed surface rupture was apparently arrested by the building and forms a left *en echelon* step around the building. The building foundation and walls were not damaged or cracked by the fault rupture.



Figure 2.25. Aerial view of a recently completed, but unoccupied, complex of six-story apartment buildings directly west of the town of Kullar. Surface rupture along the Sapanca fault segment is visible as a series of open fissures in the middle of photo.



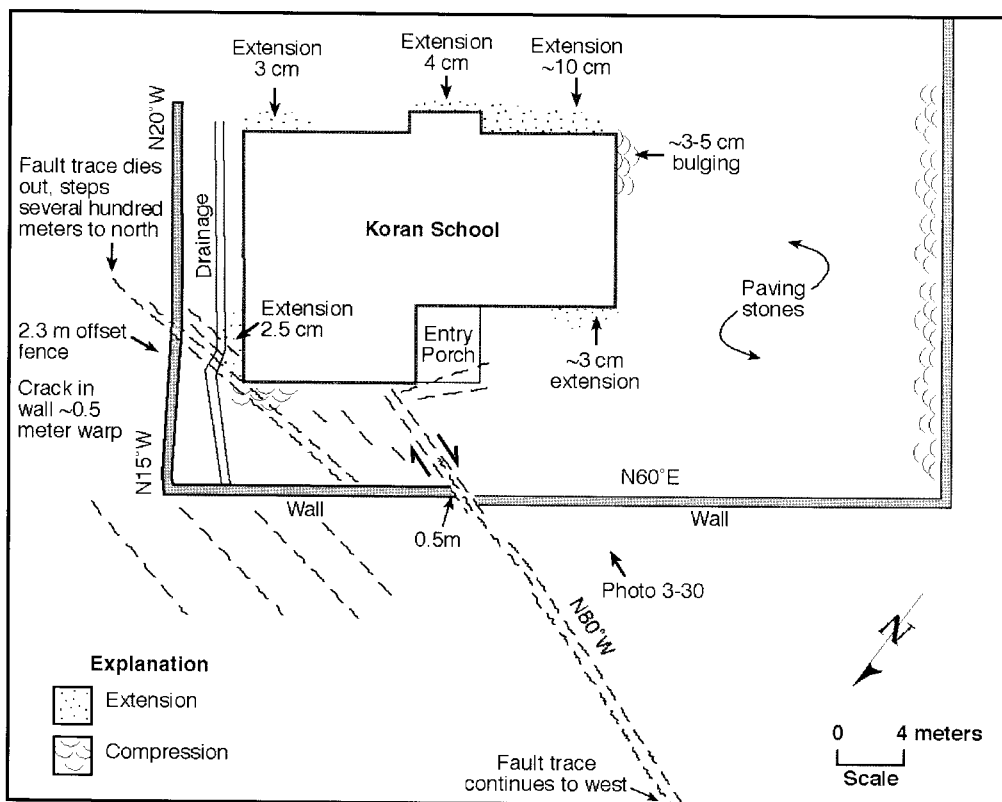
Figure 2.26. Fault rupture extended beneath the music building of a primary school in Kullar, about 4 km east of Izmit Bay. About 2 meters of lateral offset and 0.5 meter of vertical offset caused partial collapse of the school.



Figure 2.27. Fault rupture extended toward and went around a two-story concrete frame building near the damaged school in Kullar shown in figure 2.26. Approximately 1 meter of lateral offset extended to, but was arrested at, the building. Slip on the fault strand was transferred to an adjoining parallel fault strand.



Figure 2.28. Four-story concrete frame building under construction in eastern Kullar City. Fault rupture extended beneath the building, but the building foundation decoupled from soil, and the structure was not damaged.



Mapped by W. Lettis

Figure 2.29. Map of surface faulting at a Koran school along the Sapanca fault segment. Distributed fault rupture of 1 to 2 meters impacted the northern corner of the building. Rupture appears to have been stopped by the building foundation and forms a left *en-echelon* step around the building. The building rotated slightly but was not damaged.

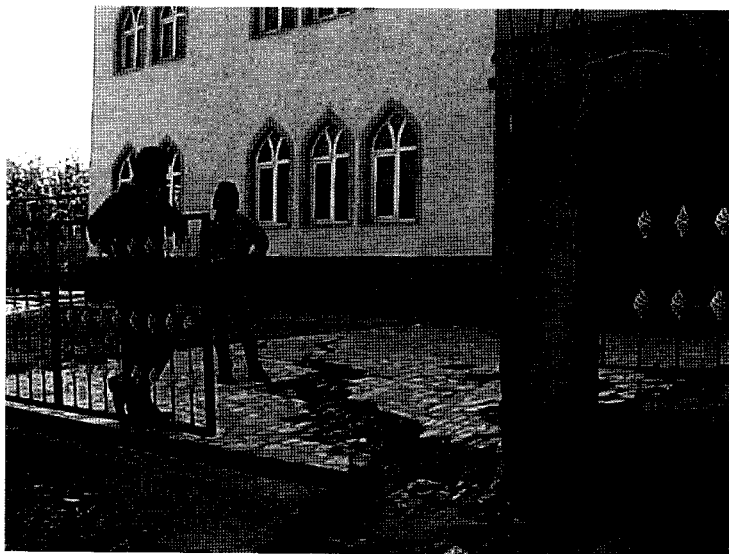


Figure 2.30. Fault rupture of about 1 meter extends toward the northern corner of the Koran school shown in figure 2.29.

Sakarya Fault Segment

Approximately 3 to 5 meters of right-lateral displacement occurred on the Sakarya fault segment (plate 1). Fault rupture extended through several small residential towns, including the town of Arifiye, and a number of agricultural communities. Within Arifiye, 3 to 3.5 meters of fault rupture extended beneath a two-story house (figures 2.31, 2.32). The house was not damaged by the fault rupture. The house foundation consisted of a shallow, 1-by-1-meter reinforced concrete grid. Apparently, the shallow foundation was sufficiently stiff and strong to hold the building intact and to allow the foundation to decouple from the underlying alluvial soil on the south side of the fault. The decoupled side at the building was dragged about 2 meters eastward by the north side of the fault. About 1 meter of lateral displacement was accommodated by compression of the soil along the margins of the house.

Directly east of Arifiye, fault rupture crossed an agricultural area, where it damaged several wood-frame structures. At one location, fault rupture caused partial collapse of three warehouses (figure 2.33). At another location, lateral offset of 5.2 meters extended the length of a tool storage shed, causing complete collapse of the building (figure 2.34).

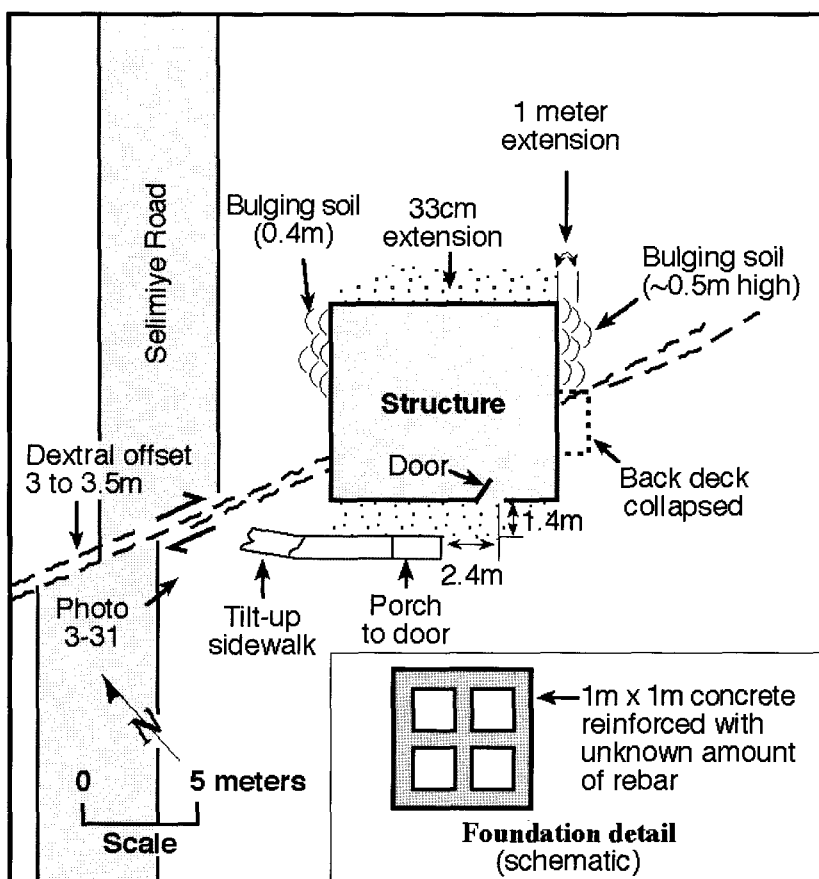


Figure 2.31. Sketch map of fault rupture beneath two-story house at #27 Selimiye Street, Arifiye, along the Sakarya fault segment.

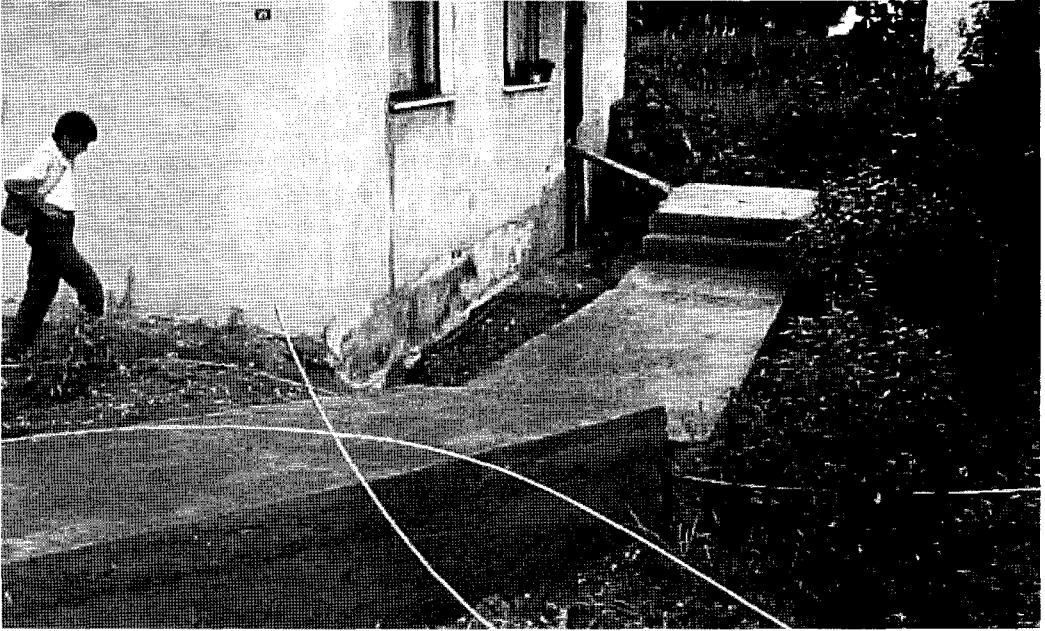


Figure 2.32. Surface faulting beneath the two-story house in figure 2.31 pulled the front porch and walkway away about 2 meters, yet the building is essentially undamaged.



Figure 2.33. Directly east of Arifiye, surface rupture of about 5 meters on the Sakarya fault segment caused partial collapse of three agriculture warehouses.

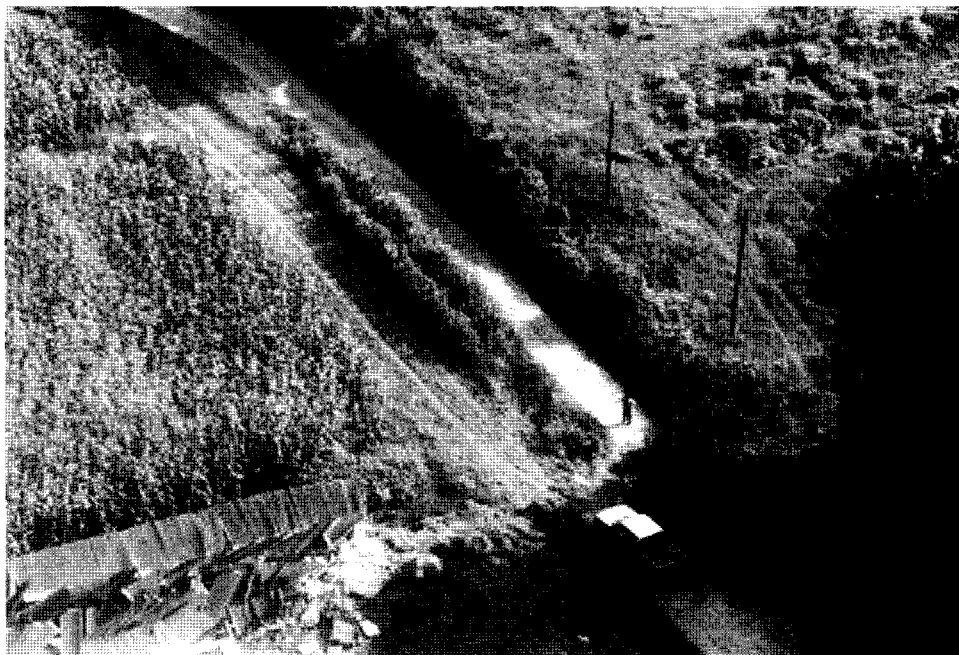


Figure 2.34. In the area of maximum offset along the Sakarya fault segment, a road is laterally offset 5.2 meters. Fault rupture extended the length of a tool storage shed and caused collapse of the shed.

Effects on Buildings Located Close to Surface Rupture

Surface fault rupture during the August 17 earthquake also passed close to numerous buildings, providing an excellent opportunity to evaluate the performance of structures near faults. Along some reaches of the fault, buildings adjacent to surface rupture completely or partially collapsed (e.g., figure 2.35). However, in several cases, if fault rupture occurred close to, but not beneath, a building foundation, the building suffered little or no observable damage. In some cases, the buildings contained fragile items such as glassware and flowerpots that remained standing, suggesting that strong ground shaking was relatively low in these areas.

For example, normal fault rupture occurred within several meters of numerous houses within the city of Gölcük and the adjoining residential area east of the city. Approximately 2.4 meters of vertical displacement occurred within 1 meter of a four-story concrete frame apartment building near the Ford-Otosan plant (figure 2.35). The building frame was undamaged by fault rupture or by strong ground shaking, although the ground deformation did produce some tilt of the building. Within the city of Gölcük, normal displacement of 1.5 meters occurred within 1 meter of a two-story house, exposing its concrete mat foundation (figure 2.36). The house was not visibly damaged by either surface fault rupture or strong ground shaking.

Lateral fault displacement also passed near several buildings on both the Sapanca and Sakarya fault segments without causing significant damage to the buildings. Figure 2.37 shows an example of fault rupture on the Sapanca segment where 3 meters of lateral slip passed within 5 to 20 meters of several two- to three-story houses. The houses were not damaged by fault rupture or by strong ground shaking. As mentioned previously, however, strong ground shaking caused significant damage to many other structures in close proximity to the fault. Thus, additional study is warranted of the possible variation of ground shaking in close proximity to the fault.



Figure 2.35. Normal fault displacement of 2.4 meters passed within 1 meter of a four-story concrete frame apartment building. The building is undamaged.



Figure 2.36. Two-story house in the city of Gölcük with 1.5-meter fault scarp. The house was not damaged.



Figure 2.37. Fault offset of 3 meters on the Sapanca fault segment. Rupture caused collapse of the house in the left foreground, but houses adjacent to the rupture were not damaged by either the fault rupture or by strong ground shaking.

EFFECTS OF SURFACE FAULT RUPTURE ON LIFELINES

Surface fault rupture caused damage to highways, water and sewer pipelines, railways, and electrical transmission lines. In many cases, fault rupture was the primary reason for closure of many transportation corridors (i.e., highways and railways) and impeded emergency response to critical areas.

Highways

The main Istanbul-Ankara highway (E80, or Trans-European Motorway) was closed at several locations by surface fault rupture, in particular, along the Sapanca and Sakarya fault segments. Where fault rupture crossed the highway, the road pavement buckled and the road was offset by up to 3 meters (figure 2.38). Near the town of Arifiye, fault rupture caused collapse of an overpass, making it necessary to close the highway for several days until debris could be removed from the roadway (figure 2.39). Highways are discussed in greater detail in the chapter on transportation systems.

Railways

Surface fault rupture caused closure of both tracks of the railroad between Izmit Bay and the town of Arifiye (figure 2.40). The tracks were damaged at several locations by lateral offset, compressional buckling, and extensional opening of the tracks. Repair crews partially opened one line within two days after the earthquake; however, repairs extended for several weeks before railway traffic could be returned to normal. The chapter on transportation includes additional discussion of earthquake effects on railways.



Figure 2.38. Fault offset of about 3 meters along the Sakarya fault segment near the town of Arifiye damaged roadways and the Trans-European Motorway.

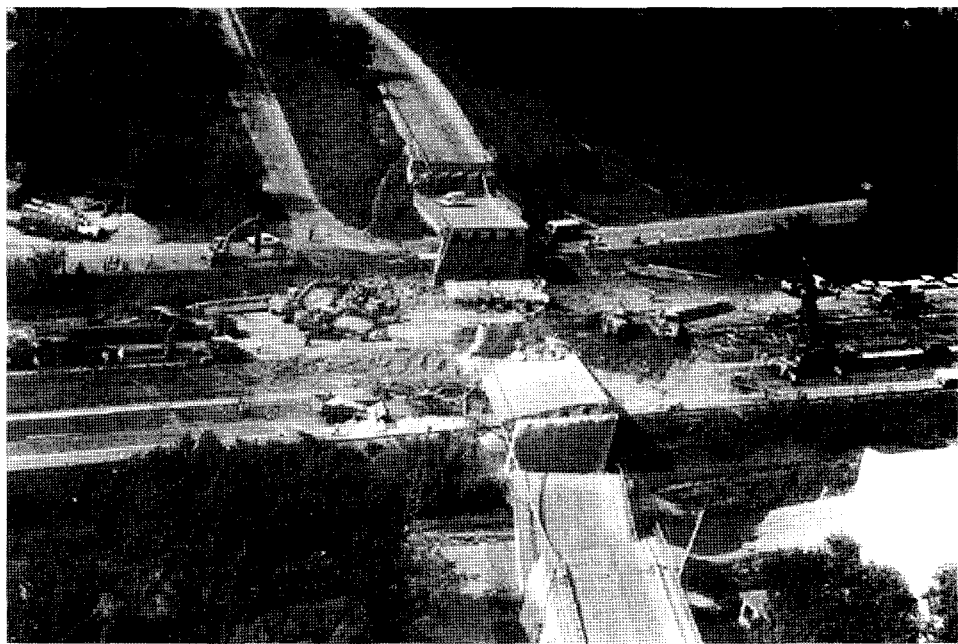


Figure 2.39. Collapse of overpass across the Trans-European Motorway (E80) near the town of Arifiye caused by 3 to 3.5 meters of right-lateral offset along the Sakarya fault segment. Collapse of the overpass caused closure of the highway for several days.

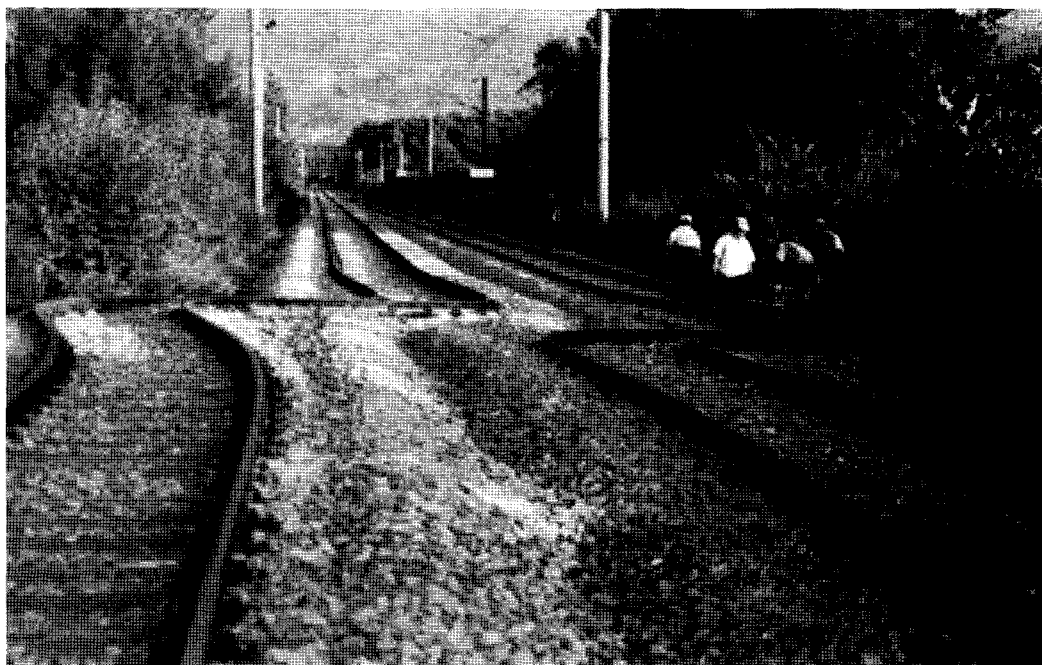


Figure 2.40. Fault rupture produced 3 meters offset of the railroad between Izmit Bay and Lake Sapanca. Repairs to the railroad opened one line within two days of the earthquake, but extended for several weeks following the earthquake.

Electrical Transmission Lines

Surface fault rupture caused only minor damage to electrical transmission lines. At one location directly east of the city of Gölcük, fault rupture of about 1.5 meters vertical and 0.5 meter lateral crossed beneath a transmission tower (figure 2.41). Rupture pulled one footing of the tower out of the soil. The footing easily decoupled from the soil because the plunge of the footing parallels the displacement of the fault in both the vertical and horizontal components. The tower essentially was undamaged because of decoupling between the tower footing and the soil.

Water Pipelines

Surface fault rupture caused significant damage to the Thames River Water pipeline system near the town of Kullar. A large-diameter (2.2 meters) Thames River main water transmission pipe crosses the Sapanca fault segment between Izmit Bay and Kullar ($40^{\circ}43.173' \text{ N}$, $29^{\circ}58.098' \text{ E}$). Between 3.16 and 3.23 meters of slip was measured by displaced walls and a fenceline west and east of the pipeline, respectively. Fault rupture did not sever the pipe but caused localized kinking of the pipe at two places and bending within a broad zone. The pipeline remained in service after the earthquake, but it suffered a significant leak at one of the kinks, which was repaired within a month of the earthquake. A field reconnaissance of the pipeline was performed on September 30, 1999, just after completion of repairs. The repaired section of the pipeline was largely backfilled at the time of the visit, with the exception of a short section near the fault crossing (pipeline Station 1+320 meters).

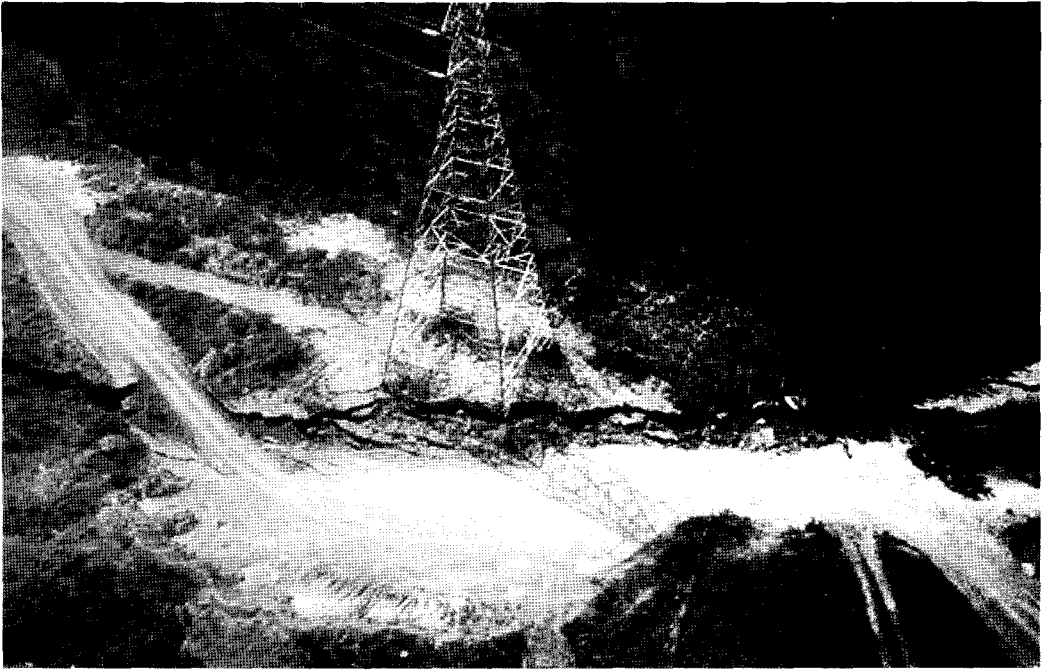


Figure 2.41. Aerial view of the normal fault along the Gölcük segment east of Gölcük, near the Ford-Otosan plant. Fault rupture crosses beneath one footing of the tower, which was pulled out of the soil, preventing damage to the tower lattice.

Following are the pipeline design specifications.

Diameter: 2,200 mm

Thickness: 18 mm

Material: Spiral welded steel (API Grade B) with field-welded butt joints

Bedding: Granular fill

Backfill: Native clay soil, compacted to minimum 30 cm over the top of the pipe

Cover: 1.5 to 2.5 meters of fill over the top of the pipe

The fault crossing occurs at a break-in-slope between an older alluvial terrace or ridge slope and a small, active alluvial valley. The pipeline descends the terrace/ridge slope at an overall trend of about N 40° W and obliquely crosses the fault zone, which has a local surface rupture trend of N 85° E (pipeline-fault angle of 55°). It is interesting to note that the fault rupture does not follow the topographic break-in-slope between the terrace/ridge and valley that trends N 68° E, but departs from the valley margin and trends obliquely up the slope east of the pipeline and over the crest of the ridge. At the fault crossing, the pipe is underlain by Holocene alluvium. Native soils exposed in the pipeline repair trench wall consist of medium stiff, dark brown clay and silty clay. Standing water was present in the trench near the bottom of the pipe and may represent either groundwater or pipe leakage. In either case, groundwater is likely to occur at shallow depth in the small alluvial valley at the crossing.

Performance of the pipe suggests that ground deformation was partially distributed plastically around the pipe, and strain was accommodated within the pipe by localized kinking and broad

bending. The primary zone of deformation in the pipe was approximately 30 meters wide and includes the two kinks and a discrete bend in the pipe. The kinks exhibited lateral displacements of up to tens of centimeters at Station 1+320 meters and Station 1+337 meters. A finger-width tear and leak occurred at the Station 1+337 meters kink, and a reported slight leak occurred at the discrete bend in the pipe at Station 1+358 meters; however, the pipe remained largely intact. The primary zone of deformation and pipe damage was localized at the fault and was surrounded by a wider zone of bending that was over 60 meters wide.

Geotechnical laboratory testing was performed on three hand-collected samples from the repair trench and adjacent to the pipeline to document site soil conditions:

1. Native clay soil (clay to silty clay with sand and fine gravel)
2. Compacted backfill (mixed native clay soil and bedding)
3. Granular bedding (well-graded gravel with silt and sand)

Results from the laboratory testing are shown in table 2.3. Native soils at the fault crossing consist of medium stiff, fat clay (CH) to silty clay with sand and fine gravel and have a plasticity index of 52% to 38%. A three-point direct shear test was performed on the native clay soil sample and indicates peak shear strength of about 44 kilopascal (kPa) at a normal stress of 29 kPa and effective stress parameters of ϕ' (phi) = 30–32° and $c' = 28$ –31 kPa. Pocket penetrometer soundings in the trench wall and backfill clay soil indicated unconfined compression strength values of between 38.6 and 76.5 kPa.

The performance of the Thames River pipeline was surprisingly good, considering that it survived approximately 3 meters of right-lateral rupture without severing. The pipe, which has a diameter–wall thickness ratio of 122:1, accommodated the displacement by discrete kinking within the 30-meter-wide primary deformation zone and broad bending through a wider zone of secondary deformation at least 60 meters wide.

SUMMARY AND CONCLUSIONS

The August 17, 1999, Kocaeli earthquake produced extensive surface rupture from the Hersek Peninsula to near the city of Düzce. The total onshore and offshore length of rupture is estimated to be 126 km. Surface rupture was primarily right-lateral strike-slip of up to 5.5 meters and averaging 3 to 4 meters. Surface rupture extended through portions of several larger cities or towns and across major transportation and lifeline corridors.

Fault rupture broke four distinct segments—the Karadere, Sakarya, Sapanca, and Gölcük—of the North Anatolian fault. These segments vary in length from 26 to 36 km and are bounded by right, *en echelon* stepovers and/or a gap in the fault trace. From east to west, the stepover and rupture gaps are Eften Lake stepover basin, Akyazi Gap and restraining bend, Lake Sapanca stepover basin, Gölcük stepover basin, and Karamürsel stepover basin. The Kocaeli rupture terminated to the west at the Karamürsel stepover basin and to the east at the Eften Lake stepover basin. Surface rupture extended across alluvial valleys north of a steep mountain front, in many places following a previously mapped fault trace characterized by geomorphic features such as degraded scarps, shutter and pressure ridges, linear drainages, sag ponds, and tectonic depressions. In other areas, the surface rupture extended across level alluvial plains that show little or no geomorphic evidence of past rupture events. A significant portion of rupture occurred offshore in Lake Sapanca and Izmit Bay.

Rupture typically was expressed as straight and *en echelon* fissures, moletracks, warped zones, and locally, vertical scarps. The primary zone was typically a few meters to about 20 meters wide, and in places it was surrounded by a broader zone of secondary deformation up to 200 meters wide. Typically 80 to 90% of the fault displacement was accommodated by one or two primary traces:

Table 2.3. Turkey, Thames River Pipeline Soil Test Results

| Smpl. No. | Material | USCS Description | Field Pocket Pen. Test (kPa) | Sieve Analyses (percent finer) | | | | Atterberg Indices | | | Natural Moisture Content | Direct Shear Peak Strength*/ Envelope |
|-----------|---|---|------------------------------|--------------------------------|--------|-------|--------|-------------------|-------|-------|--------------------------|--|
| | | | | No. 200 | No. 40 | No. 4 | 2-inch | LL | PL | PI | | |
| PF-1 | Native alluvial clay | Brown fat clay(CH) with sand and fine gravel | 38.3 to 76.5 | 75% | 87% | 95% | 100% | 73.8% | 21.5% | 52.3% | 37% | 44 kPa / $\phi' = 30^\circ$, $c = 31$ kPa |
| PF-2 | Trench backfill, compacted and mixed native soil with some granular | Brown fat clay (CH) with sand and fine gravel bedding | 38.3 to 57.4 | 52% | 66% | 88% | 100% | 58.2% | 20.2% | 37.9% | 33% | -- |
| PF-3 | Select granular bedding/shading | Brown well-graded gravel (GW) with silt and sand | -- | 7% | 18% | 51% | 100% | -- | -- | -- | -- | -- |

*Three-point, consolidated drained direct shear test. Peak strength reported for normal stress of 28.8 kPa. Friction angle and cohesion estimated from straight-line approximation of failure envelope.

locally, particularly when the fault trace deviated from the prevailing strike, rupture complexity and width increased, and 50 to 80% of displacement occurred on primary fault traces, with the rest of the deformation distributed throughout the bordering secondary zone.

Four right-lateral, extensional pull-apart basins were involved in the August 17, 1999, earthquake: the 80- to 95-km² Karamürsel basin; the 6- to 12-km² Gölcük stepover, the 7- to 14-km² Sapanca basin, and the 18- to 20-km² Eften Lake double stepover. The earthquake appears to have nucleated within the Gölcük stepover basin and ruptured bilaterally to the west and east. The Karamürsel stepover arrested about 5 meters of westward-propagating rupture, and the Eften Lake stepover arrested 1 to 1.5 meters of eastward-propagating rupture. Fault rupture of 3 meters broke through the Lake Sapanca stepover. Preliminary numerical modeling using detailed slip data from field measurements suggests that the 4 to 5 meters of slip on the Gölcük segment did not sufficiently stress the Yalova fault to cause rupture, but stress perturbation associated with 3 meters of slip on the Sapanca segment was sufficient to increase stress to the Sakarya segment across the Lake Sapanca pull-apart basin. This model agrees with field observations that fault stepovers with widths greater than 4 to 5 km can arrest up to 5 meters of fault propagation, but that 3 meters of rupture can propagate across a 1- to 2-km-wide stepover.

The August 17 fault rupture provides excellent examples of the effects of surface faulting on the built environment. Because highest priority must be given to rescue and recovery operations after a major earthquake, demolition and removal of buildings make it difficult to obtain precise data on the amount of damage due to surface fault rupture. Based on the initial reconnaissance surveys, it is estimated that about a hundred reinforced concrete frame buildings suffered partial or total collapse as a direct result of surface fault rupture through the building foundation. This number is small (but still significant) compared with the thousands of buildings that suffered similar damage due to strong ground shaking and ground failures due to liquefaction. Among the reinforced concrete buildings intersected by the primary fault trace, buildings of four or more stories typically suffered partial or total collapse. These structures pose the highest risk. One- and two-story buildings typically suffered extensive damage but did not collapse. In some cases, low buildings having shallow massive foundations that were founded on soil withstood up to 3 or 4 meters of horizontal displacement with very little or no damage to the structure. The foundations for some buildings became decoupled from the ground, allowing sliding displacement with minimal damage to the structure.

Along predominantly strike-slip sections of the fault, most of the surface displacement occurred along a very narrow (<1 to 2 meters wide) zone coincident with the primary fault traces. In these areas, damage from fault rupture was very localized and was generally restricted to the structures that were intersected by the fault. Numerous buildings built immediately adjacent to the fault rupture suffered little or no damage. Therefore, in future zoning for surface fault rupture hazard, only minimal setback from the fault may be needed where the fault trace is well defined. However, buildings adjacent to faults should be designed to accommodate a minor amount of secondary ground deformation.

Along the predominantly dip-slip section of the fault where the fault had a normal sense of displacement, the zone of deformation tended to be wider (several meters to a few tens of meters) on the downthrown (hangingwall) side of the fault, but most of the displacement occurred in a narrow zone along the main fault scarp. Numerous buildings near the fault scarp on the upthrown (footwall) side of the fault suffered little or no damage unless the foundations were intersected by the fault scarp. Where the fault scarp is well defined, setback zones can be relatively narrow on the upthrown side of the fault but should be wider on the downthrown side.

In several areas the faulting was distributed over a wide zone with no well-defined fault trace (e.g., at fault bends and at fault stepovers). Damage due to surface fault rupture occurred in these areas, but the damage tended to be much less severe.

The August 17, 1999, surface rupture occurred along a previously known active fault. In most places the main fault traces could have been identified prior to the earthquake based on detailed mapping and subsurface investigations; thus, losses due to surface fault rupture could have been mitigated. Several approaches should be considered to mitigate the hazard from future surface faulting events (Lazarte et al. 1994):

- Where possible, avoid the well-defined active fault traces.
- Where the fault traces are not well defined, limit building height to one or two stories to greatly reduce the risk of injury and loss of life.
- In areas of distributed faulting, include special provisions in building codes such as stronger foundations and one- or two-story height limits.
- Where it is impractical to avoid the fault trace, design structures to withstand fault displacement.
- Mitigate risks from surface fault rupture through advance planning for quick emergency response (e.g., proper placement of shutoff and bypass valves along pipelines and stockpiling of replacement parts).

It is not possible to eliminate all risk from fault rupture, and the tendency is for the risk to increase as population increases and urban areas continue to expand. In order to lessen the hazard, detailed maps that show the locations of active faults should be readily available to the public, and methods for mitigating the hazard should be implemented in the planning, design, and construction or retrofitting of facilities that could be affected by the active faults.

ACKNOWLEDGMENTS

Financial support for this reconnaissance effort was provided by the National Science Foundation under the Siting and Geotechnical Systems Program (Clifford Astill) and by the Pacific Earthquake Engineering Research Center (Jack Moehle). Additional support was provided by William Lettis & Associates, Inc. Pacific Gas and Electric Company (San Francisco) funded focused mapping along portions of the fault rupture to better understand the potential effect of surface fault rupture on gas and electrical systems in California. Numerous individuals mapped the extent of surface faulting following the August 17 and November 12 earthquakes. These individuals are shown as contributors to this chapter. In particular, A. Barka provided logistical support and overall compilation of surface rupture data and details regarding the Sapanca segment rupture. H. Stenner, R. Langridge, T. Fumal, and S. Christofferson mapped fault rupture along the Sakarya segment. W. Lettis, J. Bachhuber, T. Dawson, E. Altunel, J. Hengesh, Z. Cakir, A. Dikbas, and W. Page mapped fault rupture along the Gölcük and Sapanca segments and within the Gölcük, Sapanca, and Eften Lake stepovers. A. Kaya provided bathymetric data from Lake Sapanca; A. C. Güneysu provided bathymetric data from İzmit Bay. Bathymetric data was acquired from Lake Sapanca under Grant #SA-2686 from the Pacific Earthquake Engineering Center, California. J. Holmberg prepared the graphics. Personnel from the U.S. Naval Combat Camera Detachment (PH1 Bivera, PH2 L. Comer, and PH3 M. Parker) provided professional aerial camera support. Helicopter support was provided by the Department of Defense through the U.S. Marine Corps on the USS *Kearsarge* (Major Coke, Marine Helicopter Coordinator) of the 39th Air Expeditionary Squadron Operation AVID Response under the command of Colonel Chamberlain. Fakir Hüseyin Erdogan (Turkish Electricity Generation and Transmission Company) provided logistical and field support.

REFERENCES

- Ambraseys, N., and A. Zatopek. 1969. The Mudurnu Valley earthquake of July 22nd 1967. *Bulletin of the Seismological Society of America* 59 (2):521–589.
- Aydin, A., and A. Nur. 1982. Evolution of pull-apart basins and their scale independence. *Tectonics* 1 (1):91–105.
- Barka, A. A., and K. Kadinsky-Cade. 1988. Strike-slip fault geometry in Turkey and its influence on earthquake activity. *Tectonics* 7 (1):663–684.
- Barka, A., and 18 others. 1999. 17 August 1999, Izmit earthquake, Northwestern Turkey (abs.). *Eos Transactions, American Geophysical Union 1999 Fall Meeting, November 16* 80:F647.
- Berg, G. V. 1967. The Adapazari, Turkey, earthquake of July 22, 1967—a preliminary report of a field inspection for the Earthquake Inspection Project Committee. *Earthquake Engineering Research, U.S. National Academy of Engineering* 14.
- Dooley, T., and K. McClay. 1997. Analog modeling of pull-apart basins. *American Association of Petroleum Geologists Bulletin* 81 (11):1804–1826.
- Fumal, T. E., and 12 others. 1999. Slip distribution and geometry of the Sakarya section of the 1999 Izmit earthquake ground rupture, Western Turkey (abs.). *Eos Transactions, American Geophysical Union 1999 Fall Meeting, November 16* 80:F669.
- Harris, R. A., and S. M. Day. 1993. Dynamics of fault interaction: Parallel strike-slip faults. *Journal of Geophysical Research* 98 (B3):4461–4472.
- King, G. C. P., R. S. Stein, and J. Lin. 1994. Static stress changes and the triggering of earthquakes. *Bulletin of the Seismological Society of America* 84 (3):935–953.
- Lazarte, C. A., J. D. Bray, A. M. Johnson, and R. E. Lemmer. 1994. Surface breakage of the 1992 Landers earthquake and its effects on structures. *Bulletin of the Seismological Society of America* 84 (3):547–561.
- Pinar, A., D. Kalafat, G. Horasan, N. Özel, A. M. Isikara, and L. Gülen. 1999. Rupture process of the August 17, 1999, Izmit (Kocaeli) earthquake (abs.). *EOS Transactions, American Geophysical Union* 80 (46):S11D-06.
- Reches, Z. 1987. Mechanical aspects of pull-apart basins and push-up swells with applications to the Dead Sea transform. *Tectonophysics* 141:75–88.
- Segall, P., and D. D. Pollard. 1980. Mechanics of discontinuous faults. *Journal of Geophysical Research* 85 (B8):4337–4350.
- Thomas, A. L. 1993. Poly3D: A three-dimensional, polygonal element, displacement discontinuity boundary element computer program with applications to fractures, faults, and cavities in the Earth's crust. Master's thesis, Stanford University.
- Toksöz, M. N., R. E. Reilinger, C. G. Doll, A. A. Barka, and N. Yalcin. 1999. Izmit (Turkey) earthquake of 17 August 1999: First report. *Seismological Research Letters* 70 (6):669–679.
- United States Geological Survey (USGS). 2000. Implications for earthquake risk reduction in the United States from the Kocaeli, Turkey, earthquake of August 17, 1999. USGS Circular 1193.

CHAPTER CONTRIBUTORS***Coordinators***

W. Lettis

William Lettis & Associates, Inc.

J. Bachhuber

William Lettis & Associates, Inc.

R. Witter

William Lettis & Associates, Inc.

Principal Contributors

J. Bachhuber, *William Lettis & Associates, Inc.*

A. Barka, *Istanbul Technical Institute*

J. Bray, *University of California, Berkeley*

W. Lettis, *William Lettis & Associates, Inc.*

W. Page, *Pacific Gas & Electric Company*

F. Swan, *Geomatrix Consultants, Inc.*

R. Witter, *William Lettis & Associates, Inc.*

Other Contributors

E. Altunel, *Osmangazi University*

J.-P. Bardet, *University of Southern California*

R. Boulanger, *University of California, Davis*

C. Brankman, *William Lettis & Associates, Inc.*

Z. Cakir, *Istanbul Technical University*

S. Christofferson, *Southern California Earthquake Center*

L. Cluff, *Pacific Gas & Electric Company*

T. Dawson, *Southern California Earthquake Center*

T. Fumal, *U. S. Geological Survey*

A. C. Güneysu, *University of Istanbul*

J. Hengesh, *URS Corporation*

A. Kaya, *Dokuz Eylul University, Izmir*

R. Langridge, *U. S. Geological Survey*

E. Rathje, *University of Texas, Austin*

H. Stenner, *U. S. Geological Survey*